

# Cytochrome P450 Drives a HIF-Regulated Behavioral Response to Reoxygenation by *C. elegans*

Dengke K. Ma,<sup>1</sup> Michael Rothe,<sup>2</sup> Shu Zheng,<sup>1</sup> Nikhil Bhatla,<sup>1</sup> Corinne L. Pender,<sup>1</sup> Ralph Menzel,<sup>3</sup> H. Robert Horvitz<sup>2\*</sup>

Oxygen deprivation followed by reoxygenation causes pathological responses in many disorders, including ischemic stroke, heart attacks, and reperfusion injury. Key aspects of ischemia-reperfusion can be modeled by a *Caenorhabditis elegans* behavior, the O<sub>2</sub>-ON response, which is suppressed by hypoxic preconditioning or inactivation of the O<sub>2</sub>-sensing HIF (hypoxia-inducible factor) hydroxylase EGL-9. From a genetic screen, we found that the cytochrome P450 oxygenase CYP-13A12 acts in response to the EGL-9–HIF-1 pathway to facilitate the O<sub>2</sub>-ON response. CYP-13A12 promotes oxidation of polyunsaturated fatty acids into eicosanoids, signaling molecules that can strongly affect inflammatory pain and ischemia-reperfusion injury responses in mammals. We propose that roles of the EGL-9–HIF-1 pathway and cytochrome P450 in controlling responses to reoxygenation after anoxia are evolutionarily conserved.

Ischemia-reperfusion-related disorders, such as strokes and heart attacks, are the most common causes of adult deaths worldwide (1). Blood delivers O<sub>2</sub> and nutrients to target tissues, and ischemia results when the blood supply is interrupted. The restoration of O<sub>2</sub> from blood flow after ischemia, known as reperfusion, can exacerbate tissue damage (2). How organisms prevent ischemia-reperfusion injury is poorly understood. Studies of the nematode *C. elegans* led to the discovery of an evolutionarily conserved family of O<sub>2</sub>-dependent enzymes (EGL-9 in *C. elegans* and EGLN2 in mammals) that hydroxylate the HIF transcription factor and link hypoxia to hypoxia-inducible factor (HIF)-mediated physiological responses (3–7). Exposure to chronic low concentrations of O<sub>2</sub> (hypoxic preconditioning) or direct inhibition of EGLN2 strongly protects mammals from stroke and ischemia-reperfusion injury (2, 8, 9). Similarly, EGL-9 inactivation in *C. elegans* blocks a behavioral response to reoxygenation, the O<sub>2</sub>-ON response (characterized by a rapidly increased locomotion speed triggered by reoxygenation after anoxia) (10, 11), which is similar to mammalian tissue responses to ischemia-reperfusion: (i) Reoxygenation drives the O<sub>2</sub>-ON response and is the major pathological driver of reperfusion injury, (ii) hypoxic preconditioning can suppress both processes, and (iii) the central regulators (EGL-9–HIF) of both processes are evolutionarily conserved. It remains unknown how the EGL-9–HIF-1 and EGLN2–HIF pathways control the O<sub>2</sub>-ON response and ischemia-reperfusion injury, respectively.

To seek EGL-9–HIF-1 effectors important in the O<sub>2</sub>-ON response, we performed an *egl-9* suppressor screen for mutations that can restore the defective O<sub>2</sub>-ON response in *egl-9* mutants (fig. S1A). We identified new alleles of *hif-1* in this screen; because EGL-9 inhibits HIF-1, *hif-1* mutations suppress the effects of *egl-9* mutations (10). We also identified mutations that are not alleles of *hif-1* (Fig. 1, A to C, and fig. S1B). *hif-1* mutations recessively suppressed three defects of *egl-9* mutants: the defective O<sub>2</sub>-ON response, defects in egg laying, and the ectopic expression of the HIF-1 target gene *cysl-2* (previously called *K10H10.2*) (fig. S1C) (10, 12). By contrast, one mutation, *n5590*, dominantly suppressed the O<sub>2</sub>-ON defect but did not suppress the egg-laying defect or the ectopic expression of *cysl-2::GFP* (Fig. 1, D and E, and fig. S2). *n5590* restored the sustained phase (starting 30 s after reoxygenation) better than it did the initial phase (within 30 s after reoxygenation) (Fig. 1, A to C). *egl-9; hif-1; n5590* triple mutants displayed a normal O<sub>2</sub>-ON response, just like the wild type and *egl-9; hif-1* double mutants (fig. S1D). Thus, *n5590* specifically suppresses the *egl-9* defect in the sustained phase of the O<sub>2</sub>-ON response.

We genetically mapped *n5590* and identified a Met<sup>46</sup> → Ile missense mutation in the gene *cyp-13A12* by whole-genome sequencing (Fig. 2A, fig. S3A, and table S1A). Decreased wild-type *cyp-13A12* gene dosage in animals heterozygous for a wild-type allele and the splice acceptor null mutation *gk733685*, which truncates the majority of the protein, did not recapitulate the dominant effect of *n5590* (Fig. 2B). Similarly, *gk733685* homozygous mutants did not recapitulate the effect of *n5590* (Fig. 2C). Thus, *n5590* does not cause a loss of gene function. By contrast, increasing wild-type *cyp-13A12* gene dosage by overexpression restored the sustained phase of the O<sub>2</sub>-ON response (Fig. 2D), and

RNA interference (RNAi) against *cyp-13A12* abolished the effect of *n5590* (Fig. 2E). We conclude that *n5590* is a gain-of-function allele of *cyp-13A12*.

*cyp-13A12* encodes a cytochrome P450 oxygenase (CYP). CYPs can oxidize diverse substrates (13–15). The *C. elegans* genome contains about 82 CYP genes, at least two of which are polyunsaturated fatty acid (PUFA) oxygenases that generate eicosanoid signaling molecules (fig. S3B) (16, 17). On the basis of BLASTP scores, the closest human homolog of CYP-13A12 is CYP3A4 (fig. S4). We aligned the protein sequences of CYP-13A12 and CYP3A4 and found that *n5590* converts methionine 46 to an isoleucine, the residue in the corresponding position of normal human CYP3A4 (fig. S4). Methionines can be oxidized by free radicals, which are produced in the CYP enzymatic cycle, rendering CYPs prone to degradation (18, 19). Using transcriptional and translational green fluorescent protein (GFP)-based reporters, we identified the pharyngeal marginal cells as the major site of expression of *cyp-13A12* (fig. S5) and observed that the abundance of CYP-13A12::GFP protein was decreased by prolonged hypoxic preconditioning and also decreased in *egl-9* but not in *egl-9; hif-1* mutants (Fig. 2F and fig. S5). The *n5590* mutation prevented the decrease in CYP-13A12::GFP abundance by hypoxia or *egl-9*. Thus, *n5590* acts, at least in part, by restoring the normal abundance of CYP-13A12, which then promotes the O<sub>2</sub>-ON response in *egl-9* mutants.

We tested whether CYP-13A12 was normally required for the O<sub>2</sub>-ON response in wild-type animals. The *cyp-13A12* null allele *gk733685* abolished the sustained phase of the O<sub>2</sub>-ON response; the initial phase of the O<sub>2</sub>-ON response was unaffected (Fig. 3A). A wild-type *cyp-13A12* transgene fully rescued this defect (Fig. 3B). A primary role of CYP-13A12 in the sustained phase of the O<sub>2</sub>-ON response explains the incomplete rescue of the defective O<sub>2</sub>-ON response of *egl-9* mutants by *n5590* during the initial phase (Fig. 1C). The activity of most and possibly all *C. elegans* CYPs requires EMB-8, a CYP reductase that transfers electrons to CYPs (20). No non-CYP EMB-8 targets are known. The mutation *emb-8(hc69)* causes a temperature-sensitive embryonic lethal phenotype. We grew *emb-8(hc69)* mutants at the permissive temperature to the young-adult stage. A shift to the nonpermissive temperature simultaneously with *Escherichia coli*-feeding RNAi against *emb-8* nearly abolished the O<sub>2</sub>-ON response (Fig. 3, C and D). [Both the *hc69* mutation and RNAi against *emb-8* were required to substantially reduce the level of EMB-8 (17).] CYP-13A12 is thus required for the sustained phase of the O<sub>2</sub>-ON response, and one or more other CYPs likely act with CYP-13A12 to control both phases of the O<sub>2</sub>-ON response.

CYP oxygenases define one of three enzyme families that can convert PUFAs to eicosanoids, which are signaling molecules that affect inflam-

<sup>1</sup>Howard Hughes Medical Institute, Department of Biology, McGovern Institute for Brain Research, Koch Institute for Integrative Cancer Research, Massachusetts Institute of Technology, Cambridge, MA 02139, USA. <sup>2</sup>Lipidomix GmbH, Robert-Roessle-Str. 10, 13125 Berlin, Germany. <sup>3</sup>Freshwater and Stress Ecology, Department of Biology, Humboldt-Universität zu Berlin, Spaastr. 80/81, 12437 Berlin, Germany.

\*Corresponding author. E-mail: horvitz@mit.edu

matory pain and ischemia-reperfusion responses of mammals (15, 21–23); the other two families, cyclooxygenases and lipoxygenases, do not appear to be present in *C. elegans* (17, 24). To test whether eicosanoids are regulated by EGL-9 and CYP-13A12, we used high-performance liquid chromatography (HPLC) coupled with mass spectrometry (MS) to profile steady-state amounts of 21 endogenous eicosanoid species from cell extracts of wild-type, *egl-9(n586)*, and *egl-9(n586); cyp-13A12(n5590)* strains. Only free eicosanoids have potential signaling roles (21, 22, 24), so we focused on free eicosanoids. The *egl-9* mutation caused a marked decrease in the overall amount of free eicosanoids, whereas the total amount of eicosanoids, including both free and membrane-bound fractions, was unaltered (Fig. 4A and fig. S6). Among the eicosanoids profiled, 17,18-DiHEQ (17,18-diolhydroxyeicosatetraenoic acid) was the most abundant species (fig. S6B). 17,18-DiHEQ is the catabolic hydrolyase product of 17,18-EEQ (17,18-epoxyeicosatetraenoic acid), an epoxide active in eicosanoid signaling (25). Free cytosolic

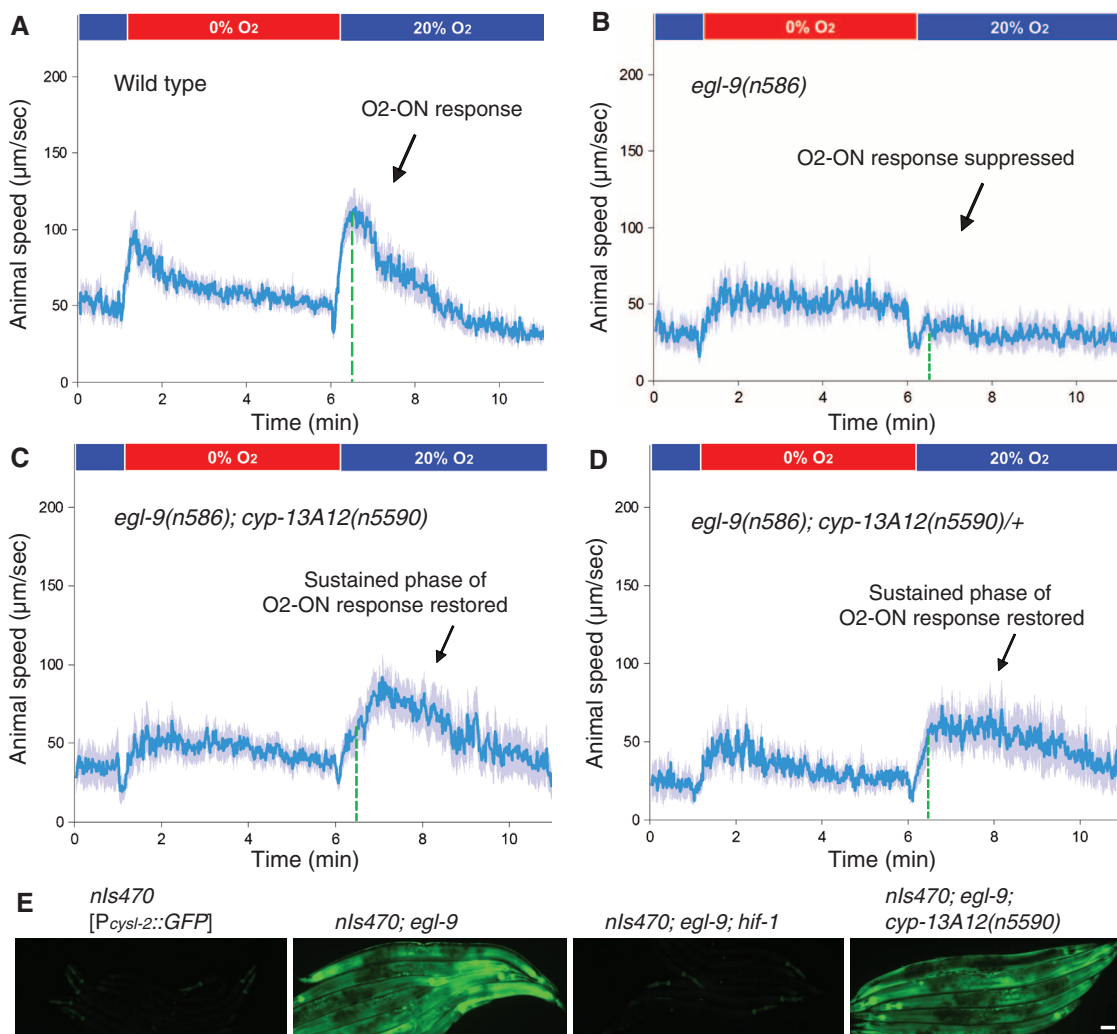
17,18-EEQ and 19-hydroxyeicosatetraenoic acid (19-HETE) were present in the wild type but undetectable in *egl-9* mutants (Fig. 4, C to F). *egl-9(n586); cyp-13A12(n5590)* mutants exhibited partially restored free overall eicosanoid levels as well as restored levels of 17,18-EEQ and 19-HETE (Fig. 4, A to F, and fig. S6B). Thus, both EGL-9 and CYP-13A12 regulate amounts of free cytosolic eicosanoids.

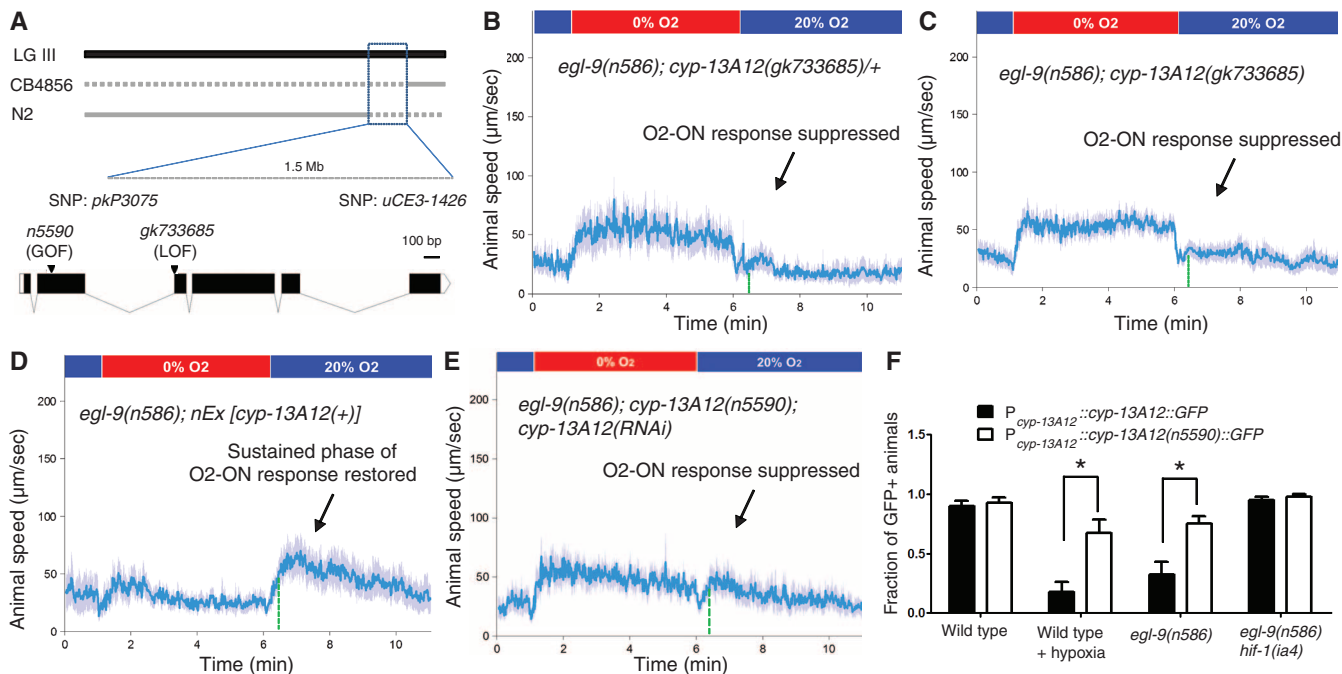
We tested whether the O<sub>2</sub>-ON response requires PUFAs, which are CYP substrates and eicosanoid precursors. PUFA-deficient *fat-2* and *fat-3* mutants (26) exhibited a complete lack of the O<sub>2</sub>-ON response, although the acceleration in response to anoxia preceding the O<sub>2</sub>-ON response was normal (Fig. 4G and fig. S7, A to C). The defective O<sub>2</sub>-ON response of *fat-2* mutants was restored by feeding animals arachidonic acid, a C20 PUFA (Fig. 4H), but not oleate, a C18 monounsaturated fatty acid that is processed by FAT-2 to generate C20 PUFAs (fig. S7D). These results demonstrate an essential role of PUFAs for the O<sub>2</sub>-ON response.

We suggest a model in which CYPs, which are strictly O<sub>2</sub>-dependent (27, 28), generate eicosanoids to drive the O<sub>2</sub>-ON response (Fig. 4I and fig. S8). In this model, EGL-9 acts as a chronic O<sub>2</sub> sensor, so that during hypoxic preconditioning, the O<sub>2</sub>-dependent activity of EGL-9 is inhibited, HIF-1 is activated, and unknown HIF-1 up-regulated targets decrease CYP protein abundance. The low abundance of CYPs defines the hypoxic preconditioned state. Without hypoxic preconditioning, CYPs generate eicosanoids, which drive the O<sub>2</sub>-ON response. By contrast, with hypoxic preconditioning or in *egl-9* mutants, the CYP amounts are insufficient to generate eicosanoids and the O<sub>2</sub>-ON response is not triggered. Neither C20 PUFAs nor over-expression of CYP-29A3 restored the defective O<sub>2</sub>-ON response of *egl-9* mutants (figs. S9 and S10), indicating that this defect is unlikely to be caused by a general deficiency in C20 PUFAs or CYPs. Because the O<sub>2</sub>-ON response requires EMB-8, a general CYP reductase, but only the sustained phase requires CYP-13A12, we propose

**Fig. 1. *n5590* suppresses the defect of *egl-9* mutants in the O<sub>2</sub>-ON response.** (A)

Speed graph of wild-type animals, showing a normal O<sub>2</sub>-ON response. Average speed values ± 2 SEM (blue) of animals (*n* > 50) are shown with step changes of O<sub>2</sub> between 20 and 0% at the indicated times. The mean speed within 0 to 120 s after O<sub>2</sub> restoration is increased relative to that before O<sub>2</sub> restoration (*P* < 0.01, one-sided unpaired *t* test). The dashed green line indicates the approximate boundary (30 s after reoxygenation) between the initial and sustained phases of the O<sub>2</sub>-ON response. (B) Speed graph of *egl-9(n586)* mutants, showing a defective O<sub>2</sub>-ON response. (C) Speed graph of *egl-9(n586); cyp-13A12(n5590)* mutants, showing a restored O<sub>2</sub>-ON response mainly in the sustained phase (right of the dashed green line). The mean speed within 30 to 120 s after O<sub>2</sub> restoration was significantly higher than that of *egl-9(n586)* mutants (*P* < 0.01). (D) Speed graph of *egl-9(n586); cyp-13A12(n5590)/+* mutants, showing a restored O<sub>2</sub>-ON response in the sustained phase. (E) *hif-1* but not *cyp-13A12(n5590)* suppressed the expression of *cysl-2::GFP* by *egl-9(n586)* mutants. GFP fluorescence micrographs of five to seven worms aligned side by side carrying the transgene *nls470* [*P<sub>cysl-2</sub>::GFP*] are shown. Scale bar, 50 μm.

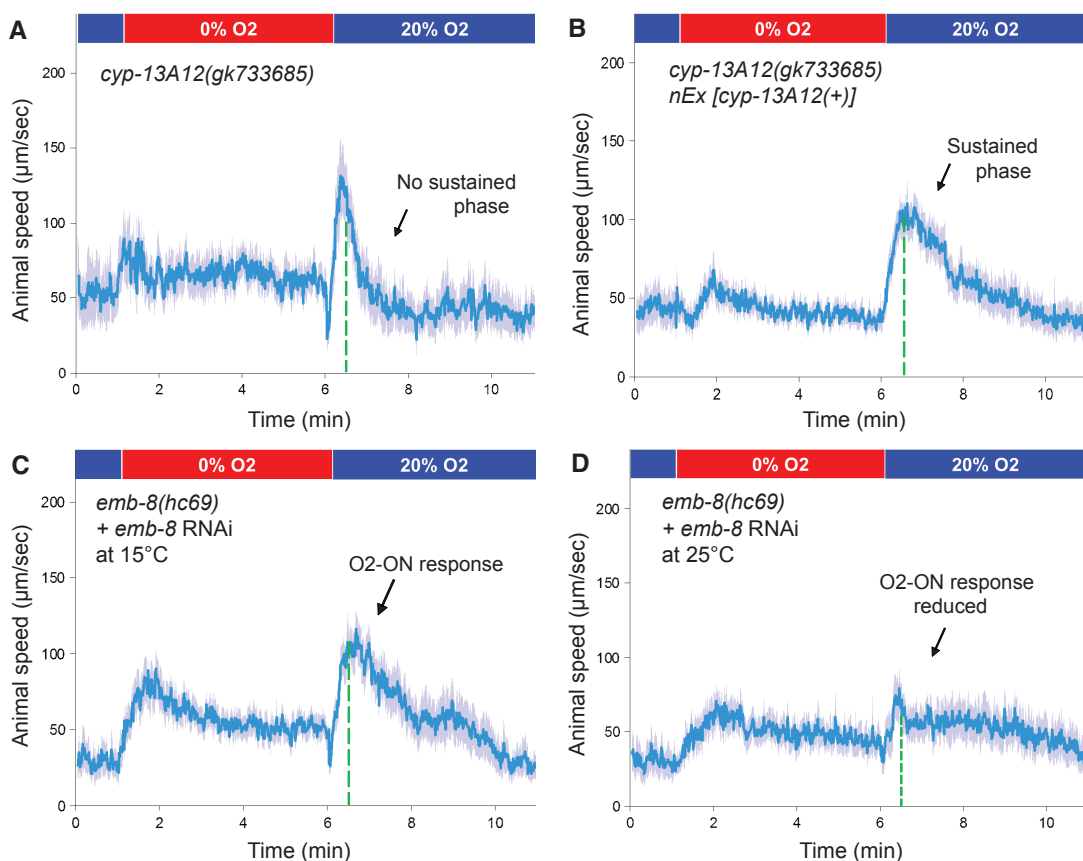




**Fig. 2. *n5590* is a gain-of-function allele of *cyp-13A12*.** (A) Genetic mapping positioned *n5590* between the SNPs *pkP3075* and *uCE3-1426*. Solid gray lines indicate genomic regions for which recombinants exhibited a defective O<sub>2</sub>-ON response, thus excluding *n5590* from those regions. The locations of *n5590* and *gk733685* are indicated in the gene diagram of *cyp-13A12*. (B) Speed graph of *egl-9(n586); cyp-13A12(gk733685)/+* animals, showing a defective O<sub>2</sub>-ON response. (C) Speed graph of *egl-9(n586);*

*cyp-13A12(gk733685)* mutants, showing a defective O<sub>2</sub>-ON response. (D) Speed graph of *egl-9(n586); nEx [cyp-13A12(+)]* animals, showing a restored O<sub>2</sub>-ON response in the sustained phase (right of the dashed green line). (E) Speed graph of *egl-9(n586); cyp-13A12(n5590); cyp-13A12(RNAi)* animals, showing a suppressed O<sub>2</sub>-ON response. (F) Fractions of animals expressing CYP-13A12::GFP or CYP-13A12(*n5590*)::GFP [*\*P* < 0.01, two-way analysis of variance (ANOVA) with Bonferroni test, *n* = 4].

**Fig. 3. Requirement of CYP-13A12 for a normal O<sub>2</sub>-ON response.** (A) Speed graph of *cyp-13A12(gk733685)* loss-of-function mutants, showing an O<sub>2</sub>-ON response with a normal initial phase but a diminished sustained phase (left and right, respectively, of the dashed green line). (B) Speed graph of *cyp-13A12(gk733685)* mutants with a rescuing wild-type *cyp-13A12* transgene, showing the O<sub>2</sub>-ON response with a normal initial phase and sustained phase. The mean speed within 30 to 120 s after O<sub>2</sub> restoration was higher than that of *cyp-13A12(gk733685)* mutants (*P* < 0.01, one-sided unpaired *t* test, *n* > 50). (C) Speed graph of *emb-8(hc69)* mutants grown at the permissive temperature of 15°C with simultaneous *E. coli*-feeding RNAi against *emb-8*, showing a normal O<sub>2</sub>-ON response. (D) Speed graph of *emb-8(hc69)* mutants grown post-embryonically at the restrictive temperature of 25°C with simultaneous *E. coli*-feeding RNAi against *emb-8*, showing a reduced O<sub>2</sub>-ON response.



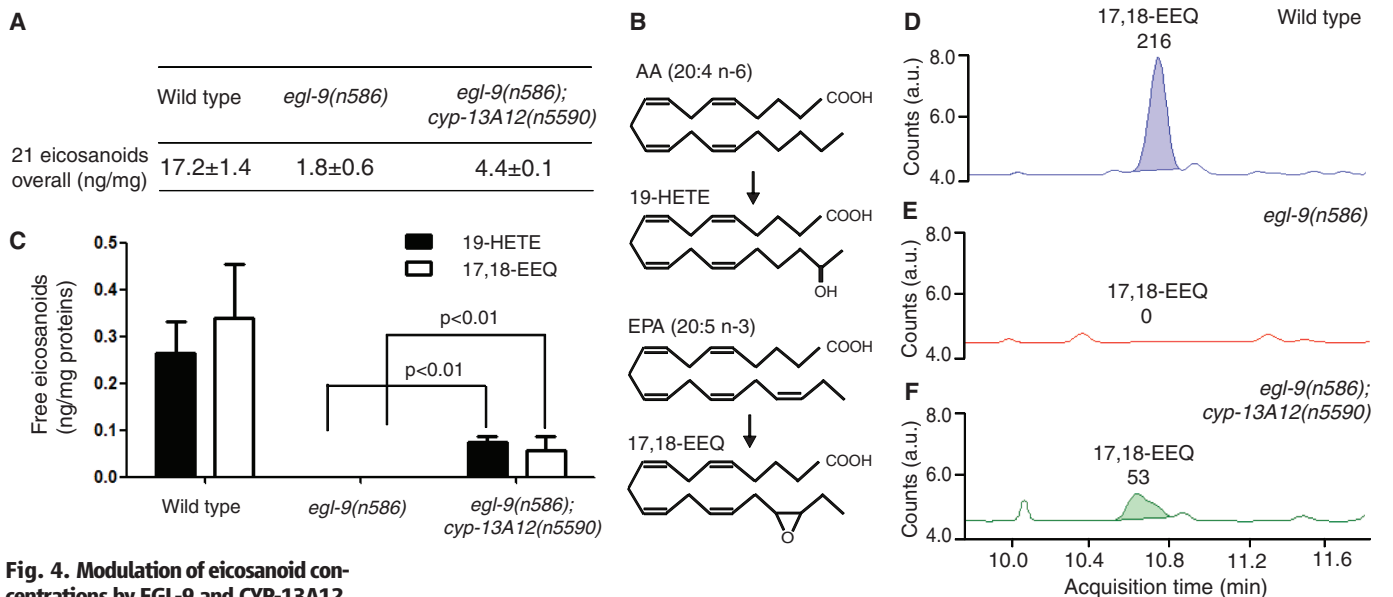
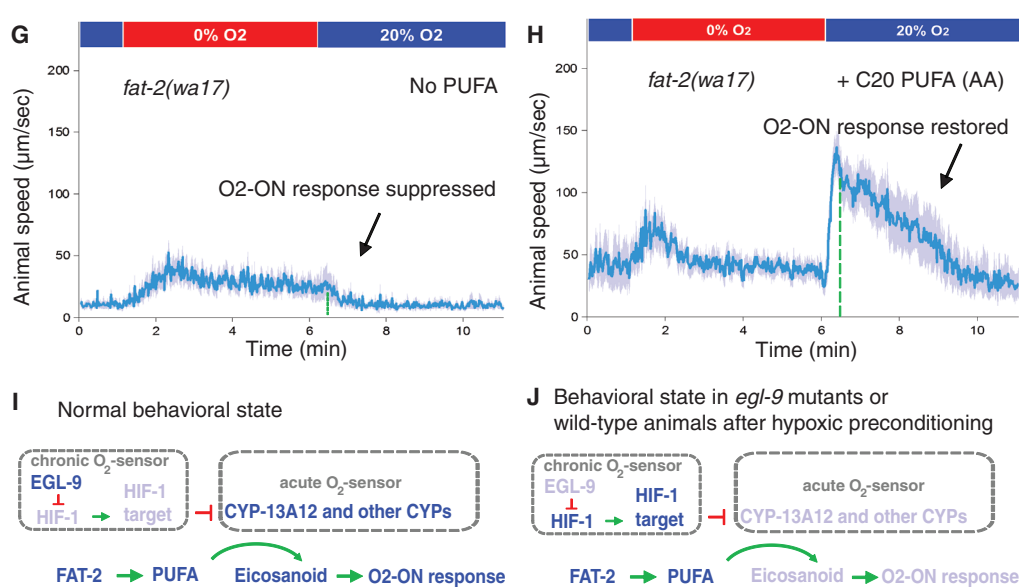


**Fig. 4. Modulation of eicosanoid concentrations by EGL-9 and CYP-13A12.**

(A) Overall levels of free eicosanoids, calculated by adding the values of the profiled 21 eicosanoids in the wild type and in the *egl-9(n586)* and *egl-9(n586); cyp-13A12(n5590)* strains. (B) Schematic illustrating the conversion of arachidonic acid (AA) to 19-HETE and of eicosapentaenoic acid (EPA) to 17,18-EEQ by CYPs. (C) Quantification of 19-HETE and 17,18-EEQ concentrations in the wild type and in *egl-9(n586); cyp-13A12(n5590)* and *egl-9(n586)* mutant strains. Amounts of free (membrane-unbound) forms of 17,18-EEQ and 19-HETE from extracts of age-synchronized young adult hermaphrodites are shown ( $P < 0.01$ , two-way ANOVA post hoc test,  $n = 3$ ). Error bars are SEM. (D to F) Representative HPLC-MS traces indicating free 17,18-EEQ levels based on the spectrograms of three MS samples: (D) wild type, (E) *egl-9(n586)*, and (F) *egl-9(n586); cyp-13A12(n5590)*. Peaks of 17,18-EEQ



at its transition  $m/z$  (mass-to-charge ratio) were measured and extracted (MassHunter). The  $x$  axis shows the retention time (minutes); the  $y$  axis shows the abundance (counts), with specific integral values over individual peaks indicated above each peak. (G) Speed graph of *fat-2* mutants, showing a defective O<sub>2</sub>-ON response. Animals were supplemented with the solvents used in (H) as a control. (H) Speed graph of *fat-2* mu-

tants, showing the O<sub>2</sub>-ON response rescued by C20 PUFA (AA) supplementation. (I and J) Model of how EGL-9 and CYPs control the O<sub>2</sub>-ON response under (I) normoxic conditions and (J) conditions of hypoxic preconditioning or in *egl-9* mutants (see text for details). Light blue indicates low protein activity, low amounts of eicosanoids, or a defective O<sub>2</sub>-ON response.

that CYP-13A12 and other CYPs act as acute O<sub>2</sub> sensors and produce eicosanoids, which are short-lived and act locally (22) during reoxygenation to signal nearby sensory circuits that drive the O<sub>2</sub>-ON response.

In humans, a low uptake of PUFAs or an imbalanced ratio of ω3-to-ω6 PUFAs is associated with elevated risk of stroke, cardiovascular disease, and cancer (21, 23, 29, 30). Cytochrome P450s and eicosanoid production also have been implicated in mammalian ischemia-reperfusion (15, 21). Nonetheless, little is known concerning the causal relationships among and mechanisms relating O<sub>2</sub> and PUFA homeostasis, CYP, and

PUFA-mediated cell signaling and organismal susceptibility to oxidative disorders. Our results identify a pathway in which EGL-9–HIF-1 regulates CYP-eicosanoid signaling, demonstrate that PUFAs confer a rapid response to reoxygenation via CYP-generated eicosanoids, and provide direct causal links among CYPs, PUFA-derived eicosanoids, and an animal behavioral response to reoxygenation. Because the molecular mechanisms of O<sub>2</sub> and PUFA homeostasis are fundamentally similar and evolutionarily conserved between nematodes and mammals (7, 11, 26), we suggest that the *C. elegans* O<sub>2</sub>-ON response is analogous to the mammalian tissue and cellular

response to ischemia-reperfusion injury and that the molecular pathway including EGL-9–HIF-1 and CYPs in controlling responses to reoxygenation after anoxia is evolutionarily conserved.

**References and Notes**

1. A. S. Go *et al.*, *Circulation* **127**, e6–e245 (2013).
2. H. K. Eltzschig, T. Eckle, *Nat. Med.* **17**, 1391–1401 (2011).
3. A. C. Epstein *et al.*, *Cell* **107**, 43–54 (2001).
4. W. G. Kaelin Jr., P. J. Ratcliffe, *Mol. Cell* **30**, 393–402 (2008).
5. C. Trent, N. Tsuing, H. R. Horvitz, *Genetics* **104**, 619–647 (1983).
6. G. L. Semenza, *Cell* **148**, 399–408 (2012).
7. J. A. Powell-Coffman, *Trends Endocrinol. Metab.* **21**, 435–440 (2010).

8. G. L. Semenza, *Biochim. Biophys. Acta* **1813**, 1263–1268 (2011).
9. J. Aragonés *et al.*, *Nat. Genet.* **40**, 170–180 (2008).
10. D. K. Ma, R. Vozdek, N. Bhatla, H. R. Horvitz, *Neuron* **73**, 925–940 (2012).
11. D. K. Ma, N. Ringstad, *Front. Biol.* **7**, 246–253 (2012).
12. M. W. Budde, M. B. Roth, *Genetics* **189**, 521–532 (2011).
13. D. R. Nelson *et al.*, *Pharmacogenetics* **6**, 1–42 (1996).
14. O. Gotoh, *Mol. Biol. Evol.* **15**, 1447–1459 (1998).
15. R. A. Gottlieb, *Arch. Biochem. Biophys.* **420**, 262–267 (2003).
16. M. Kosel *et al.*, *Biochem. J.* **435**, 689–700 (2011).
17. J. Kulas, C. Schmidt, M. Rothe, W. H. Schunck, R. Menzel, *Arch. Biochem. Biophys.* **472**, 65–75 (2008).
18. B. S. Berlett, E. R. Stadtman, *J. Biol. Chem.* **272**, 20313–20316 (1997).
19. R. C. Zangar, D. R. Davydov, S. Verma, *Toxicol. Appl. Pharmacol.* **199**, 316–331 (2004).
20. C. A. Rappleye, A. Tagawa, N. Le Bot, J. Ahringer, R. V. Aroian, *BMC Dev. Biol.* **3**, 8 (2003).
21. J. Szefer *et al.*, *Curr. Mol. Med.* **11**, 13–25 (2011).
22. M. P. Wymann, R. Schneider, *Nat. Rev. Mol. Cell Biol.* **9**, 162–176 (2008).
23. R. S. Chapkin, W. Kim, J. R. Lupton, D. N. McMurray, *Prostaglandins Leukot. Essent. Fatty Acids* **81**, 187–191 (2009).
24. D. Panigrahy, A. Kaipainen, E. R. Greene, S. Huang, *Cancer Metastasis Rev.* **29**, 723–735 (2010).
25. C. Arnold *et al.*, *J. Biol. Chem.* **285**, 32720–32733 (2010).
26. J. L. Watts, *Trends Endocrinol. Metab.* **20**, 58–65 (2009).
27. D. R. Harder *et al.*, *Circ. Res.* **79**, 54–61 (1996).
28. J. P. Ward, *Biochim. Biophys. Acta* **1777**, 1–14 (2008).
29. M. Gerber, *Br. J. Nutr.* **107** (suppl. 2), S228–S239 (2012).
30. D. Mozaffarian, J. H. Wu, *J. Am. Coll. Cardiol.* **58**, 2047–2067 (2011).

**Acknowledgments:** We thank C. Bargmann, A. Fire, A. Hart, Y. Iino, J. Powell-Coffman, and C. Rongo for reagents and the *Caenorhabditis* Genetics Center and the Million Mutation Project for strains. H.R.H. is an Investigator of the Howard Hughes Medical Institute. Supported by NIH grant GM24663 (H.R.H.), German Research Foundation grant ME2056/3-1 (R.M.), a NSF Graduate Research Fellowship (N.B.), the MIT Undergraduate Research Opportunities Program (S.Z.), and a Helen Hay Whitney Foundation postdoctoral fellowship (D.K.M.).

**Supplementary Materials**

www.sciencemag.org/cgi/content/full/science.1235753/DC1  
 Materials and Methods  
 Supplementary Text  
 Figs. S1 to S11  
 Table S1  
 References (31–70)

28 January 2013; accepted 10 June 2013  
 Published online 27 June 2013;  
 10.1126/science.1235753

# Robustness and Compensation of Information Transmission of Signaling Pathways

Shinsuke Uda,<sup>1</sup> Takeshi H Saito,<sup>1</sup> Takamasa Kudo,<sup>1</sup> Toshiya Kokaji,<sup>2</sup> Takaho Tsuchiya,<sup>1</sup> Hiroyuki Kubota,<sup>1</sup> Yasunori Komori,<sup>1</sup> Yu-ichi Ozaki,<sup>1\*</sup> Shinya Kuroda<sup>1,2,3,†</sup>

Robust transmission of information despite the presence of variation is a fundamental problem in cellular functions. However, the capability and characteristics of information transmission in signaling pathways remain poorly understood. We describe robustness and compensation of information transmission of signaling pathways at the cell population level. We calculated the mutual information transmitted through signaling pathways for the growth factor–mediated gene expression. Growth factors appeared to carry only information sufficient for a binary decision. Information transmission was generally more robust than average signal intensity despite pharmacological perturbations, and compensation of information transmission occurred. Information transmission to the biological output of neurite extension appeared robust. Cells may use information entropy as information so that messages can be robustly transmitted despite variation in molecular activities among individual cells.

Signaling pathways transmit signals from growth factors to downstream gene expression, influencing various cell fate decisions such as cell differentiation (1). To control cellular responses by stimulation intensity, signaling pathways must reliably transmit stimulation intensity through their signaling activities. The reliability of signal transmission depends on the balance between signal intensity and variation. The smaller the signal variation, the more information can be transmitted through a pathway with the same dynamic range of signal in-

tensity. Even high-intensity signals cannot be reliably transmitted if the variation in signal intensity is large. In contrast, even signals with low intensity can be reliably transmitted if the variation in signal intensity is small (Fig. 1A). Thus, the reliability of signal transmission depends on both average (mean) intensity and variation. As a consequence, the number of controllable states of cellular responses is determined by the number of reliably transmitted signals. Intuitively, the larger the number of reliably transmitted signals, the more information the signal pathway can transmit. If cellular signaling pathways are treated as communication channels in the framework of Shannon’s information theory (2–12), the amount of information that can be reliably transmitted through a cellular signaling pathway can be measured by mutual information, which corresponds to the logarithm of the average number of controllable states of a cellular response that can be defined by varied upstream signals (13–15).

We evaluated the information transmission from growth factors to the immediate early genes (IEGs) through various signaling pathways in PC12 cells. Nerve growth factor (NGF), pituitary

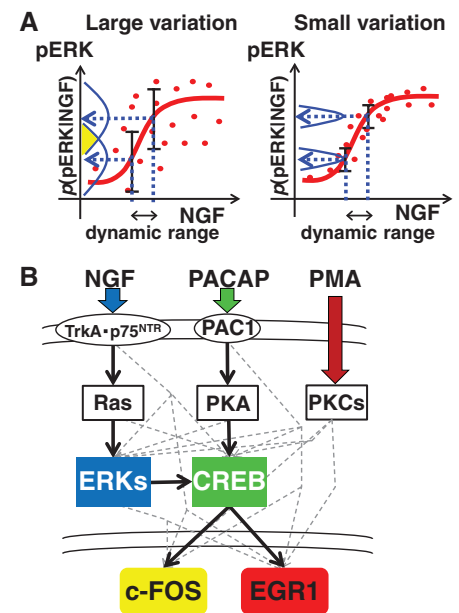


**Fig. 1. Information transmission of signaling pathways.** (A) Reliability of information transmission depends on both signal intensity and variation. More information can be transmitted with the same dynamic range of signal intensity if signal variation is smaller. Dots denote intensities of pERKs in individual cells, and lines denote the average intensity of pERKs.  $p(\text{pERKs}|\text{NGF})$  denotes the distribution (a normalized histogram) of pERKs for a given dose of NGF. (B) Signaling pathways from growth factors, such as NGF, PACAP, and PMA to the IEGs, such as c-FOS and EGR1. Solid lines indicate the reported pathways for each growth factor, and gray dashed lines indicate other possible pathways. The colored boxes are the measured molecules, and white ovals are unmeasured molecules in this study.

<sup>1</sup>Department of Biophysics and Biochemistry, Graduate School of Science, University of Tokyo, Bunkyo-ku, Tokyo 113-0033, Japan. <sup>2</sup>Department of Computational Biology, Graduate School of Frontier Sciences, University of Tokyo, Bunkyo-ku, Tokyo 113-0033, Japan. <sup>3</sup>CREST, Japan Science and Technology Corporation, Bunkyo-ku, Tokyo 113-0033, Japan.  
 \*Present address: Quantitative Biology Center, RIKEN, 6-2-3, Furuedai, Suita, Osaka 565-0874, Japan.  
 †Corresponding author. E-mail: skuroda@bi.s.u-tokyo.ac.jp



## Supplementary Materials for

### **Cytochrome P450 Drives a HIF-Regulated Behavioral Response to Reoxygenation by *C. elegans***

Dengke K. Ma, Michael Rothe, Shu Zheng, Nikhil Bhatla, Corinne L. Pender, Ralph Menzel,  
H. Robert Horvitz\*

\*Corresponding author. E-mail: horvitz@mit.edu

Published 27 June 2013 on *Science Express*  
DOI: 10.1126/science.1235753

**This PDF file includes:**

Materials and Methods

Supplementary Text

Figs. S1 to S11

Table S1

References

## Materials and Methods

### EMS Mutagenesis, Genetic Screens, Mapping and Whole-genome Sequencing

To screen for *egl-9* suppressors, we mutagenized *egl-9(n586)* mutants carrying the *cysl-2::GFP* transgene *nIs470* with ethyl methanesulfonate (EMS) and observed the F2 progeny in one of three ways using: (1) a dissecting microscope and GFP fluorescence to isolate suppressors of *cysl-2::GFP* overexpression, (2) a dissecting microscope to isolate suppressors of the defective egg-laying behavior, and (3) a compound microscope and a nitrogen gas-flow chamber to isolate suppressors of the defective O<sub>2</sub>-ON response.

We refer to mutations that cause diminished *cysl-2::GFP* fluorescence or restored egg-laying behavior under conditions of normoxia (21% O<sub>2</sub>) as GFP or Egl suppressors, respectively. To isolate suppressors of the defective O<sub>2</sub>-ON response of *egl-9* mutants, we used a nitrogen gas-flow chamber system with a 100% nitrogen gas source, flow-meters, and a lid with gas tubing inlets and outlets mounted on a Petri plate freshly seeded with *E. coli* OP50 (10). Animals with restored rapid acceleration immediately (0 - 60s) after reoxygenation (by removal of the plate lid) were identified as suppressors of the defective O<sub>2</sub>-ON response. False positives were eliminated by retesting animals in the next generation using a population assay (>50 animals) (10).

To map the *egl-9* suppressor mutation *n5590*, we first generated a polymorphic Hawaiian *egl-9(n586)* strain by repeatedly crossing *egl-9(n586)* with the Hawaiian wild-type strain CB4856. *nIs470; egl-9(n586); n5590* mutants were then crossed with the Hawaiian *egl-9(n586)* strain for genetic mapping. F2 animals were isolated, and clonal F3 populations were assayed for the O<sub>2</sub>-ON response. Mapping using SNP analysis (50)

positioned *n5590* between the SNPs *pkP3075* and *uCE3-1426* on chromosome III (Fig. 2A).

Whole-genome sequencing and data analyses were performed as described (51). Two protein-coding mutations were identified in the *n5590* interval defined above: a T-to-G mutation in the gene *Y39E4A.2* and a G-to-A mutation in the gene *cyp-13A12*. As described in the text, we showed that the *egl-9* suppressor *n5590* is a gain-of-function mutation of *cyp-13A12*.

### Behavioral Analyses

The O<sub>2</sub>-ON response was measured using a multi-worm tracker with a gas-flow chamber system and quantified by customized MatLab algorithms as previously described (10). For experiments using the C20 PUFA arachidonic acid as a food supplement, arachidonic acid salts (Cayman Chemical) were dissolved in ethanol at 1 mg/ml, and 50  $\mu$ L was spread evenly onto NGM plates before drying briefly and cultivating OP50 *E. coli* on the plates. *C. elegans* was then transferred to the PUFA-supplemented plates.

To quantify egg-laying behavior, we scored the developmental stages of newly laid eggs of young adult hermaphrodites that had been transferred to fresh NGM plates with OP50 (52).

### Determination of eicosanoid levels

Endogenous CYP-derived eicosanoids were assayed for the N2 wild-type strain as well as for *egl-9(n586)* and *egl-9(n586); cyp-13A12(n5590)* mutant strains. For each experiment (three independent cultures per strain), 12,000 stage-synchronized larvae were allocated to four fresh Petri plates (diameter = 94 mm) and further cultivated at 22.5 °C until the young adult stage (24 hrs post-L4). To generate a synchronous culture of first-stage (L1) larvae, a population of well-fed animals was collected from Petri plates by rinsing and then filtered through a 10 µm membrane (SM 16510/11, Sartorius, Goettingen, Germany), a pore size that retains all but L1 larvae. These larvae were allowed to grow to be young adults and then were filtered again to eliminate L1 larvae of the next generation and so retain exclusively young adults. Subsequently, animals were prepared for LC-MS/MS analysis essentially as described previously (17). Briefly, aliquots corresponding to 30 mg wet weight were mixed with internal standard compounds (10 ng each of 20-HETE-d6, 14,15-EET-d8 and 14,15-DHET-d11; from Cayman Chemicals, Ann Arbor, MI, USA) and either subjected to alkaline hydrolysis (total eicosanoids) or directly extracted with methanol/water (free eicosanoids) followed by solid-phase extraction of the metabolites. Sample preparation, HPLC and MS conditions as well as the monitoring of multiple reactions for the analysis of the CYP-eicosanoid profile were as described previously (25). The protein concentration of each sample was measured after hydrolysis (53).

### Mutations and Strains

*C. elegans* strains were cultured as described previously (54). The N2 Bristol strain (54) was used as the reference wild-type strain, and the polymorphic Hawaiian

strain CB4856 (55) was used for genetic mapping and SNP analysis. Mutations used were as follows: LG III, *cyp-13A12(n5590 and gk733685)* (*gk733685* was obtained from the Million Mutation Project (56)), *emb-8(hc69)* (20), *cdk-5(ok626)* (41); LG IV, *fat-2(wa17)*, *fat-3(wa22, ok1126)* (57); LG V, *egl-9(sa307, n586)* (5, 58), *hif-1(ia4, n5513, n5527)* (59, 60).

Transgenic strains were generated by germline transformation as described (61). Transgenic constructs were co-injected (at 20 - 50 ng/μl) with mCherry reporters, and lines of mCherry-positive animals were established. Gamma irradiation was used to generate integrated transgenes. Transgenic strains used were as follows: *nEx2015* [*P<sub>cyp-13A12</sub>::GFP; P<sub>unc-54</sub>::mCherry*]; *nEx2016* [*P<sub>cyp-13A12</sub>::cyp-13A12::GFP; P<sub>unc-54</sub>::mCherry*]; *nEx2017* [*cyp-13A12(+)*]; *nEx2018* [*cyp-13A12(n5590)*]; *nIs587* [*P<sub>cyp-13A12</sub>::GFP; P<sub>unc-54</sub>::mCherry*]; *nIs588* [*P<sub>cyp-13A12</sub>::cyp-13A12::GFP; P<sub>unc-54</sub>::mCherry*]; *nIs589* [*P<sub>cyp-13A12</sub>::cyp-13A12(n5590)::GFP; P<sub>unc-54</sub>::mCherry*]; *nIs470* [*P<sub>cysl-2</sub>::GFP; P<sub>myo-2</sub>::mCherry*].

### Molecular biology

Constructs were generated using the PCR-fusion technique (62), the Gateway system (Invitrogen) and the Infusion cloning (Clontech) technique (63). Primer sequences are shown in Table S1.

### Statistical analyses

One-sided unpaired t-tests were used to compare the mean speeds of all animals within 60 or 120 seconds before or after O<sub>2</sub> restoration (10).  $p < 0.01$  indicates speed differences that are significant, as noted in each figure. Fisher's exact tests were used after egg-laying behavioral assays to compare the distributions of the six categories of embryos from the wild type and various mutants. Two-way ANOVA was used to calculate p values to test for significance of the effects of genotypes and different conditions in the O<sub>2</sub>-ON response.

### Bioinformatics

The BLASTP program from NCBI was used to search for proteins homologous to CYP-13A12 (64). Multiple sequence alignments were generated and analyzed using ClusterW2 (65), and the results were displayed and annotated using JalView (66). Schematic gene structures and annotations were generated using the Exon-Intron Graphic Maker (<http://wormweb.org/exonintron>).

### **Supplementary Text**

Transcriptional and translational GFP reporters with the *cyp-13A12* promoter or with the promoter and coding sequence were both most strongly expressed in the pharynx (fig. S5). The GFP-stained pharyngeal cells extended processes along the anterior pharyngeal bulb and exhibited finger-like protrusions, and we identified these cells as the pharyngeal marginal cells (MCs). MCs intercalate with pharyngeal muscles and might

structurally reinforce these muscles (31). However, MCs contain abundant mitochondria, suggesting that these cells might perform active non-structural roles (32). The O<sub>2</sub>-ON response involves rapid reoxygenation and occurs independently of known aerotactic neural O<sub>2</sub> sensors (10, 11, 33-35); we hypothesize that MCs actively signal reoxygenation by converting PUFAs to membrane-diffusible eicosanoids, which are sensed by nearby sensory neurons and trigger the O<sub>2</sub>-ON response via neural circuits that control forward/backward locomotion (36, 37).

In *egl-9* mutants or animals with prolonged (24 hrs) hypoxic preconditioning (10), the O<sub>2</sub>-ON response is suppressed because CYP-13A12 is decreased through the EGL-9/HIF-1 pathway (Figs. 2F and 4J). Our GFP reporter experiments indicate that regulation of CYP-13A12 by EGL-9/HIF-1 occurs primarily by regulation of the abundance of CYP proteins (Fig. 2F and fig. S5). HIF-1 activation can facilitate protein ubiquitination and homeostasis and pro-survival effects of hypoxic preconditioning likely require suppression of protein translation in *C. elegans* (38-40). We suggest that one or more transcriptional targets of HIF-1 regulate the abundance of CYP-13A12 and likely that of other CYPs, since CYP-13A12 does not control the initial phase but EMB-8, a general CYP reductase, affects both the initial and sustained phases (Fig. 3). *egl-9(n685); cyp-13A12(n5590)* mutants might have been restored for the sustained phase of the O<sub>2</sub>-ON response because they have restored the abundance of CYP-13A12 and thus partially restored the ability to produce eicosanoids from PUFAs. Because *cdk-5* mutations suppress the defective LIN-10 trafficking in *egl-9* mutants (41), we also tested *cdk-5* mutants and found that *cdk-5* mutations did not suppress *cysl-2::GFP* expression, the defective egg-laying behavior, or the defective O<sub>2</sub>-ON response or of *egl-9* mutants (figs.

S11A-S11B), indicating that EGL-9 regulates the O<sub>2</sub>-ON response independently of CDK-5.

Our conclusions are consistent with findings that mammalian CYP proteins closely related to *C. elegans* CYP13A12 are expressed in tissues that display ischemia-reperfusion injury and are involved in eicosanoid signaling. For example, CYP3A4 is the most closely related human homolog of *C. elegans* CYP13A12 (162/501 or 32% amino acid identity with CYP13A12) and is mainly expressed in the liver but is also highly expressed in the brain (42-44), consistent with our hypothesis that CYP3A4 modulates ischemic processes in these organs. We note that members of particular CYP protein families share high similarity in general, and CYP13A12 is also homologous to other mammalian CYPs, including the CYP5A1 thromboxane synthase (148/481 or 31% amino acid identity with CYP13A12), which generates the eicosanoid thromboxane and is widely expressed in the vasculature (45), suggesting that CYP5A1-generated eicosanoids function in the vasculature. Increased production of HETE-type eicosanoids is also associated with ischemia-reperfusion processes (46, 47). The modulation of ischemia-reperfusion by CYPs in mammals is thus unlikely mediated by a single CYP, such as CYP3A4, just as the O<sub>2</sub>-ON response of *C. elegans* is likely mediated by one or more other CYPs in addition to CYP-13A12. Rather, we suggest that the principle of CYP-mediated regulation and the novel molecular pathway including EGL-9/HIF-1 and CYPs in regulating responses to anoxia-reoxygenation are conserved; different mammalian CYPs might act in different tissues and organs. The observation that potent inhibitors of CYPs, such as sulfaphenazole, cause strong protection against ischemia-reperfusion injury (15, 48, 49) is consistent with our model. Using *C. elegans* genetics and a

behavioral model of ischemia/reperfusion, we demonstrate a direct causal role of CYPs in the response to anoxia-reoxygenation and therefore suggest a similarly causal role of CYPs in modulating mammalian ischemia-reperfusion processes.

Supplementary Figures

fig. S1

A

*nls470 IV; egl-9(n586) V*  
(*cysl-2::GFP+*, Egl and defective O<sub>2</sub>-ON response)

↓ EMS

F1

↓

F2 single animals examined

Three classes of suppressor mutants:

i, CYSL-2::GFP: GFP-

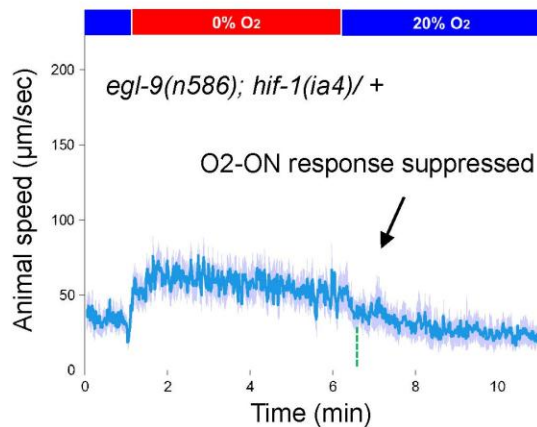
ii, Egg laying: non-Egl

iii, Locomotion: O<sub>2</sub>-ON defect restored

B

Class	<i>nls470; egl-9</i> suppressor	GFP	Egg-laying	O <sub>2</sub> -ON
i	none	GFP+	Egl	Defective
	<i>n5601</i>	GFP-	Egl	Defective
	<i>n5602</i>			
	<i>n5603</i>			
	<i>n5604</i>			
	<i>n5605</i>			
ii	<i>n5454</i>	GFP+	Non-Egl	Defective
	<i>n5607</i>			
	<i>n5608</i>			
iii	<i>n5460</i>	GFP+	Egl	Normal
	<i>n5609</i>			
	<i>n5590</i>			

C



D

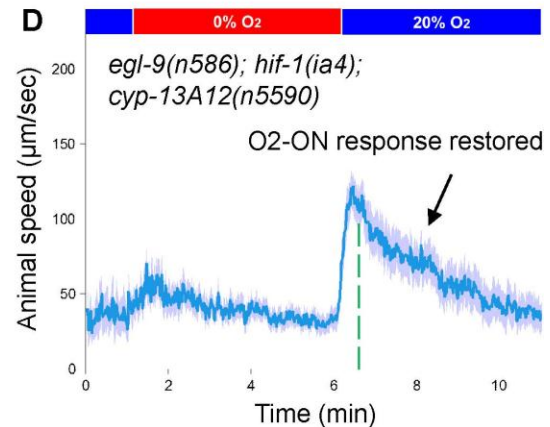


**fig. S1. Genetic screens for *egl-9* suppressors**

(A) Schematic of the screens for *egl-9* suppressors. Approximately 15,000 haploid genomes were screened. (B) Summary of the non-*hif-1* suppressor mutant isolates, showing that each of the three aspects of the *egl-9* mutant phenotype was separately suppressed. (C) Speed graph of *egl-9; hif-1/+* mutants with a defective O2-ON response, showing the recessive suppression of *egl-9* by *hif-1*. Cross progeny of *egl-9; hif-1* and *egl-9* mutants were assayed for the O2-ON response. (D) Speed graph of *egl-9(n586); hif-1(ia4); cyp-13A12(n5590)* triple mutants, showing a normal O2-ON response. Canonical alleles of *egl-9* and *hif-1* were used.

fig. S2

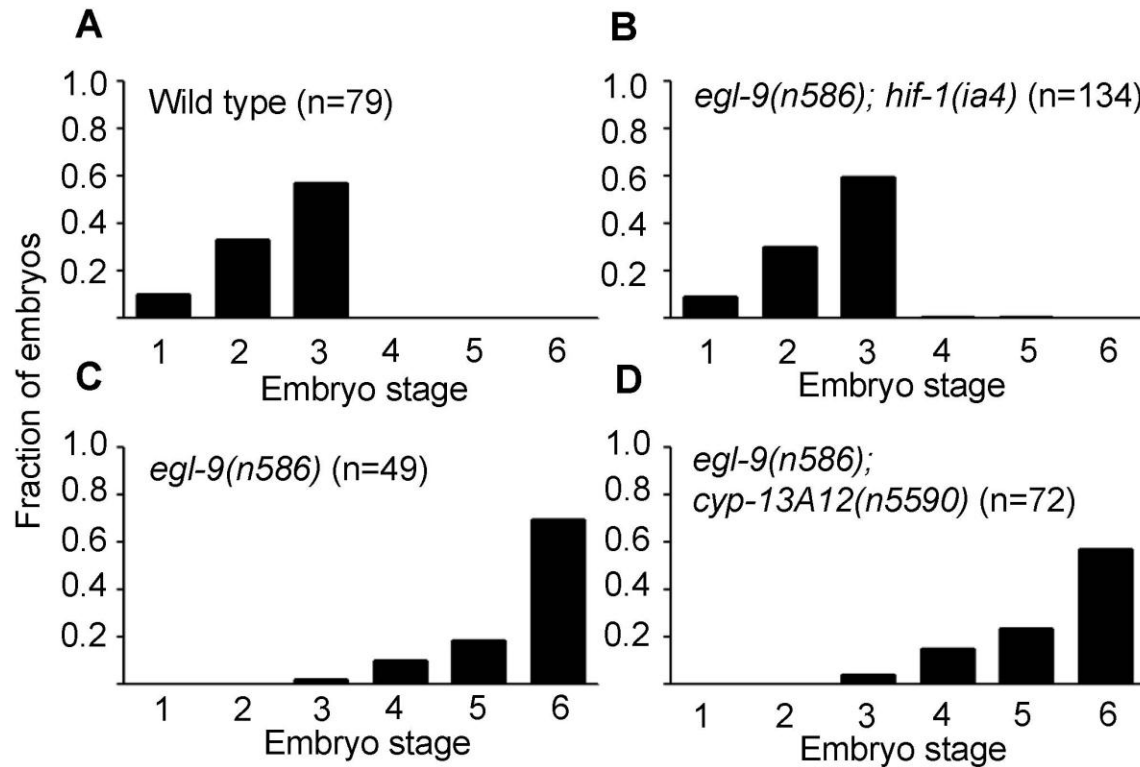


**fig. S2. *n5590* did not suppress the defective egg-laying of *egl-9* mutants**

(A-D) *hif-1* but not *cyp-13A12(n5590)* suppressed the egg-laying defect of *egl-9(n586)* mutants ( $p < 0.001$ , Fisher's exact test). Fractions of the developmental stages of eggs laid by animals carrying various mutations are shown.

**A**

transmembrane domain [cytochrome P450 catalytic domain...]

MAIIFLAILTSIIGVLSFYLVWTWSYWKRRGIAGPSGYPILGSALEMLSSENPPYLQLKE  
 WTKQYGKVVYGITEGLSRTLVIDPDLVQEVFVKQYDNFFGRKLNPIQGDPNKDKRVNLFSSQGHR  
 WKRLRTISSPTFSNNSLRKLTVEECAVELLRHIEQHTDGGQPIDLLDFYQEFTLDVIGRIAMGQT  
 DSQMFKNPLL PYVRAVFGEPKGLFLSGSLAPWIGPILRMVMFSLPNIVKNPAVHVIRHTSNAVEQ  
 RVKLRMADEKAGIDPGEPQDFIDLFLDAKSDDVELENNEDFTKAGVKVTRQLTTEEIVGQCFVFLI  
 AGFDTTALSLSYSSFLATHPKVQKQLQEEIDRECADPEVTFDQLSKLKYMECVIKETLRMYPLGA  
 LANSRCCMRATKIGNYEIDEGTNILCDTWTLHSDKSIWGEDAEFEFKPERWESGDEHFYQKGGYIP  
 FGLGPRQCIGMRLAYMEEKLLLSHILRKYTLEVCNKTQIPLKLIQSRTTQPESVWLNLTTPRDDN  
 ...cytochrome P450 catalytic domain]

**B**

Human CYP gene family	<i>C. elegans</i> CYPs	Known <i>C. elegans</i> functions
CYP1 and CYP2	CYP-14A1 to A5 CYP-22A1 (DAF-9) CYP-23A1 CYP-33A1 CYP-33B1 CYP-33C1 to C12 CYP-33D1 to D3 CYP-33E1 CYP-33E2 CYP-33E3 CYP-34A1 to A10 CYP-35A1 to A5 CYP-35B1 to B3 CYP-35C1 CYP-35D1 CYP-35E1 to E3 CYP-36A1	PCB hydroxylase? steroidogenic or fatty acid hydroxylase          PUFA hydroxylase  PCB hydroxylase?
CYP3	CYP-13A1 to A12 CYP-13B1 to B2 CYP-25A1 to A5 CYP-43A1	
CYP4	CYP-29A1 to A2 CYP-29A3 CYP-31A2 to A3 CYP-32A1-B1 CYP-37A1-B1 CYP-42A1	PUFA hydroxylase
CYP11, CYP24 and CYP27	CYP-44A1	

**fig. S3. The predicted catalytic CYP domain of CYP-13A12 and its protein family homology**

(A) Primary structure of CYP-13A12, which is predicted by SOSUI (67) to be membrane-spanning with the C-terminal end in the cytoplasm. The membrane-spanning segment is indicated with red, the predicted CYP domain is indicated with blue and the methionine residue mutated in *cyp-13A12(n5590)* is indicated with green. (B) Four

categories of predicted *C. elegans* CYP genes based on their amino acid sequence similarities to human counterparts. Known biochemical functions for CYP-22A1 (a.k.a. DAF-9), CYP-33E2 and CYP-29A3 as lipid hydroxylases are noted (16, 17, 68, 69).

fig. S4

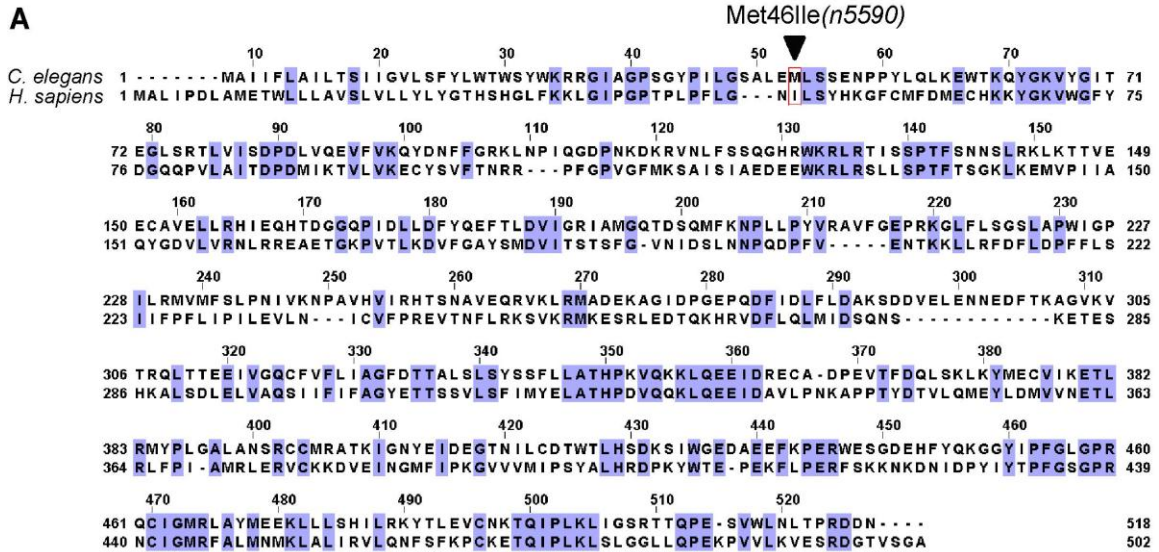
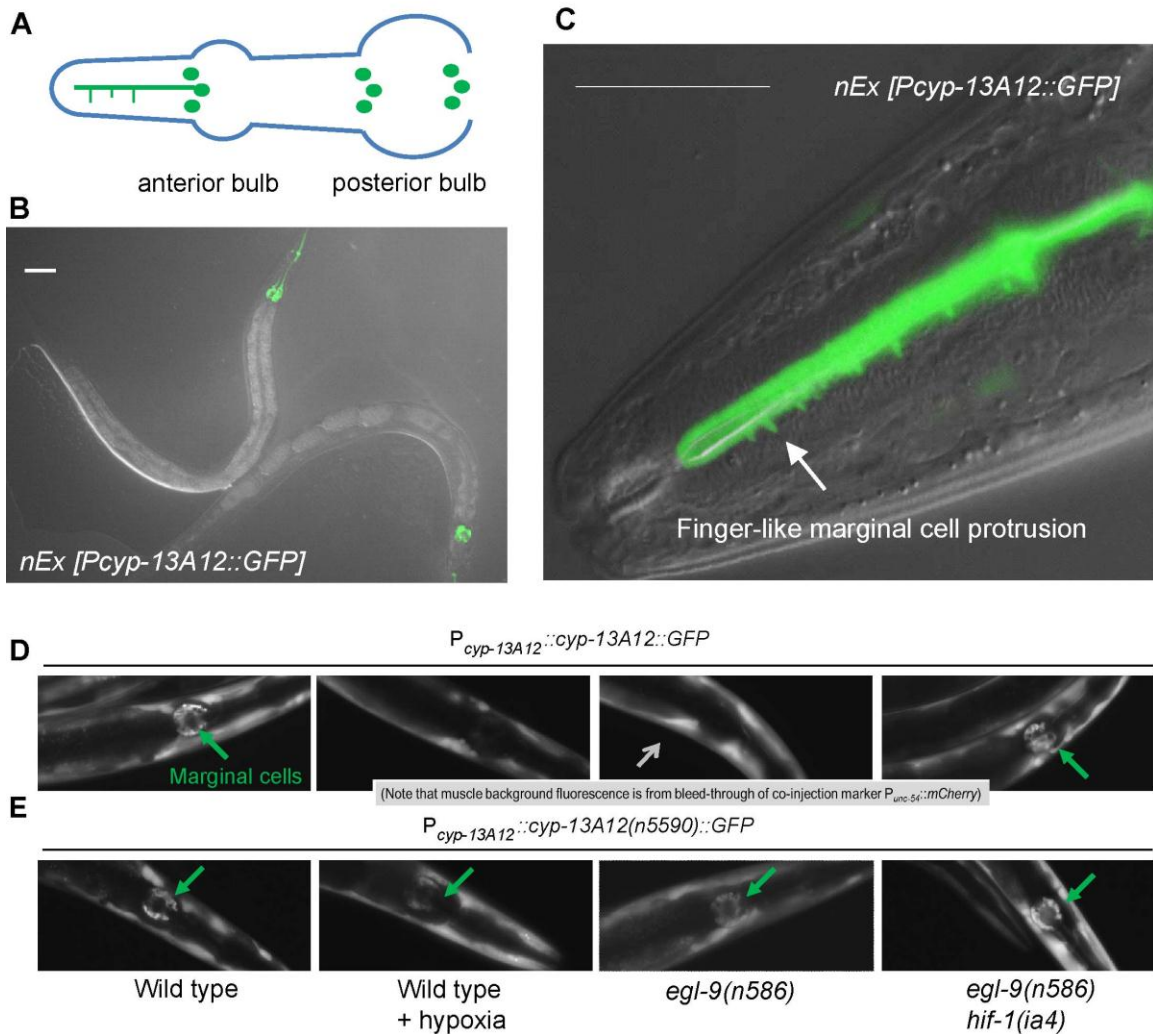


fig. S4. Similarity between *C. elegans* CYP-13A12 and human CYP3A4 proteins

(A) Protein sequence alignment showing homology between CYP-13A12 and human CYP3A4. The arrowhead indicates the *n5590* Met46Ile mutation.

fig. S5



**fig. S5. Expression pattern of *cyp-13A12* and effects of hypoxia, *cyp-13A12(n5590)* and *egl-9* mutations on CYP-13A12**

(A) A diagram of the *C. elegans* pharynx, showing the locations of the nuclei of the nine marginal cells (green). The process of one anterior marginal cell is shown with tiny protrusions that intercalate with pharyngeal muscles. (B) Merged image of Nomarski and GFP fluorescence micrographs showing expression of *cyp-13A12* in the pharynx. Scale bar, 50  $\mu$ m. The transcriptional reporter used was an extrachromosomal array of genotype

*nEx [P<sub>cyp-13A12</sub>::GFP]*. (C) Merged image of high-magnification Nomarski and GFP fluorescence micrographs showing expression of *cyp-13A12* in a marginal cell with finger-like protrusions, one of which is indicated by the arrow. Unlike translational reporters (see below), patterns or levels of GFP expression in such *cyp-13A12* transcriptional reporters are not significantly altered by hypoxic preconditioning or *egl-9* mutations. (D) Representative fluorescence micrographs indicating expression of a *P<sub>cyp-13A12</sub>::cyp-13A12::GFP* transgene of translational fusion protein in various strains or after 24 hrs hypoxic preconditioning (10). The reporter contains the promoter and genomic coding regions of *cyp-13A12* fused with GFP. Note that CYP-13A12::GFP proteins, which were present in marginal cells (green arrows), were down-regulated by hypoxia and in *egl-9* mutants, compared with in wild-type animals. (E) Representative fluorescence micrographs indicating expression of a *P<sub>cyp-13A12</sub>::cyp-13A12(n5590)::GFP* transgene of translational fusion protein in various strains or after 24 hrs hypoxic preconditioning. CYP-13A12(M46I)::GFP proteins were not down-regulated by hypoxia or in *egl-9* mutants. Equal exposure times were used. Also note that the background fluorescence from body wall muscles (grey arrow) corresponds to fluorescence emission bleed-through from the co-injection marker *P<sub>unc-54</sub>::mCherry*. The background fluorescence is not present in the transcriptional reporter because the transcriptional GFP reporter is at least one magnitude brighter than the translational GFP reporter.

fig. S6

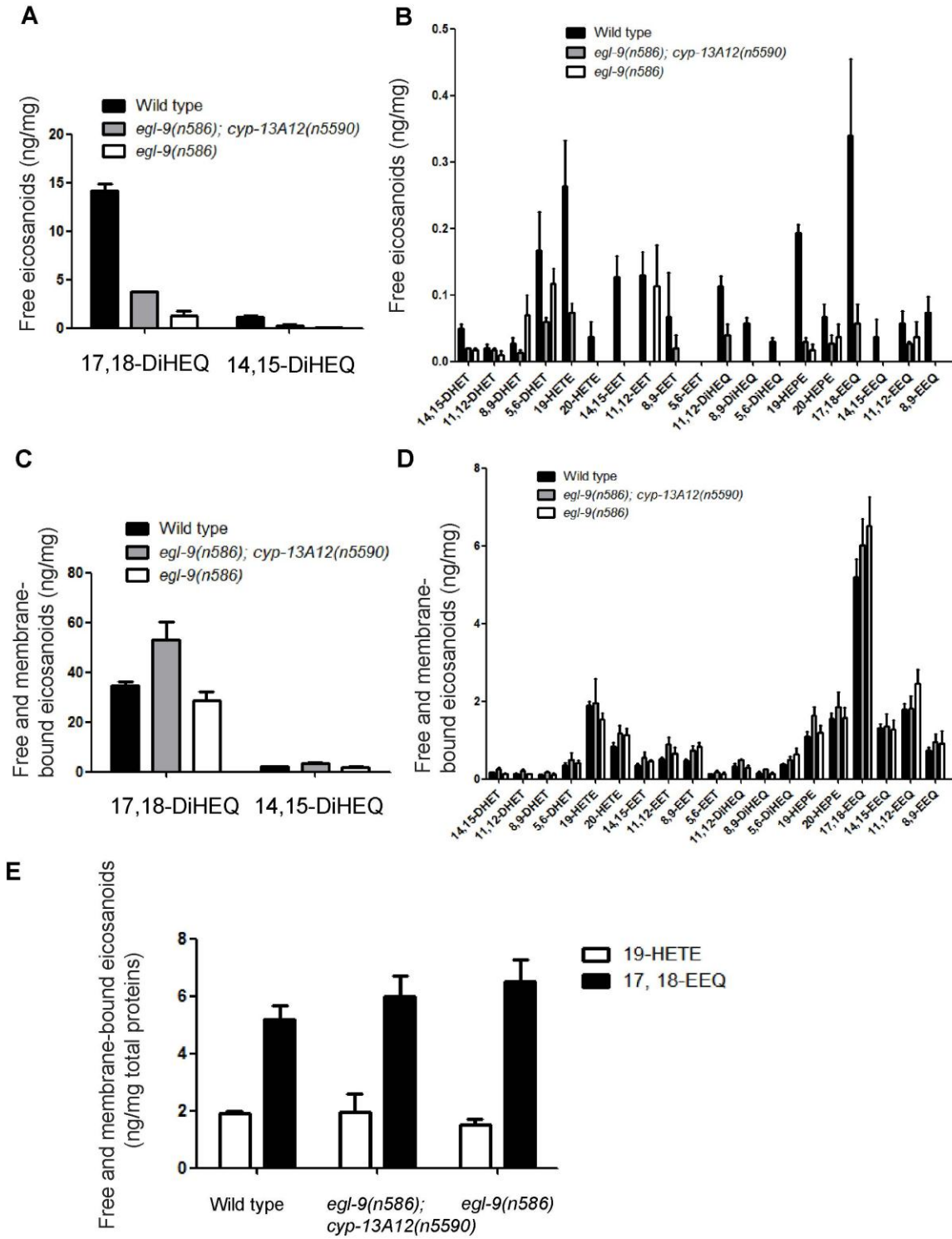


**fig. S6. EGL-9 and CYP-13A12-regulated eicosanoids**

(A) Levels of free (membrane-unbound) 17,18-DiHEQ and 14,15-DiHEQ profiled by HPLC/MS. (B) Levels of free (membrane-unbound) 14,15-DHET, 11,12-DHET, 8,9-DHET, 5,6-DHET, 19-HETE, 20-HETE, 14,15-EET, 11,12-EET, 8,9-EET, 5,6-EET, 11,12-DiHEQ, 8,9-DiHEQ, 5,6-DiHEQ, 19-HEPE, 20-HEPE, 17,18-EEQ, 14,15-EEQ, 11,12-EEQ, and 8,9-EEQ profiled by HPLC/MS. (C) Levels of total (both free and membrane-bound) 17,18-DiHEQ and 14,15-DiHEQ profiled by HPLC/MS. (D) Levels of total (both free and membrane-bound) 14,15-DHET, 11,12-DHET, 8,9-DHET, 5,6-DHET, 19-HETE, 20-HETE, 14,15-EET, 11,12-EET, 8,9-EET, 5,6-EET, 11,12-DiHEQ, 8,9-DiHEQ, 5,6-DiHEQ, 19-HEPE, 20-HEPE, 17,18-EEQ, 14,15-EEQ, 11,12-EEQ, and 8,9-EEQ profiled by HPLC/MS. (E) Levels of total 17,18-EEQ and 19-HETE profiled by HPLC/MS. Error bars, SEMs, n = 3.

fig. S7

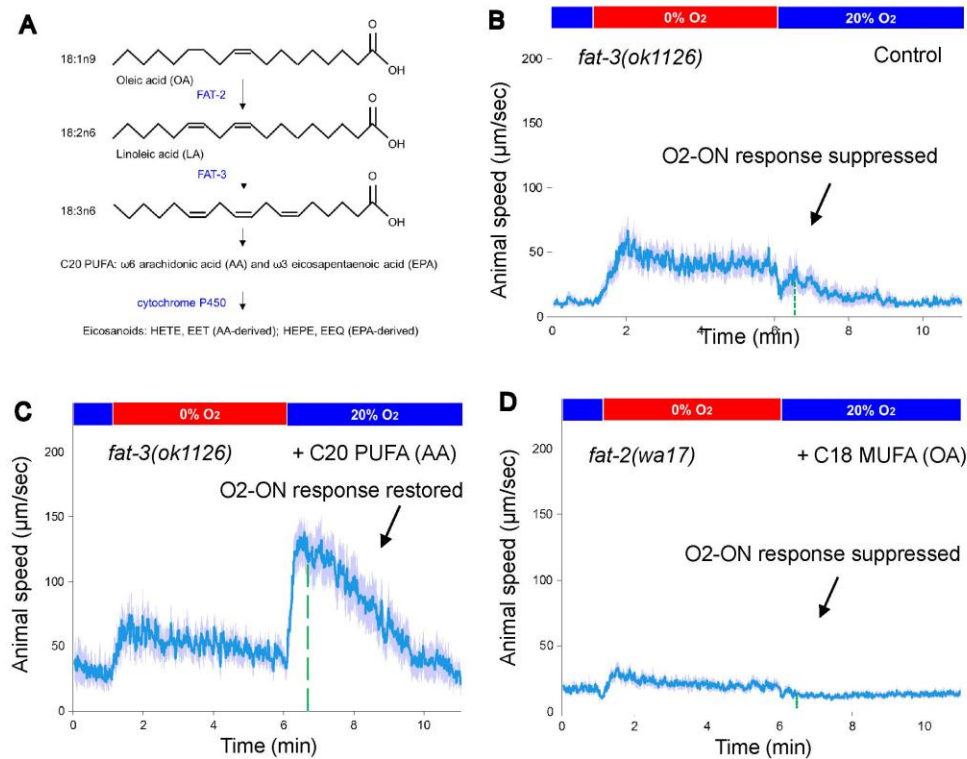
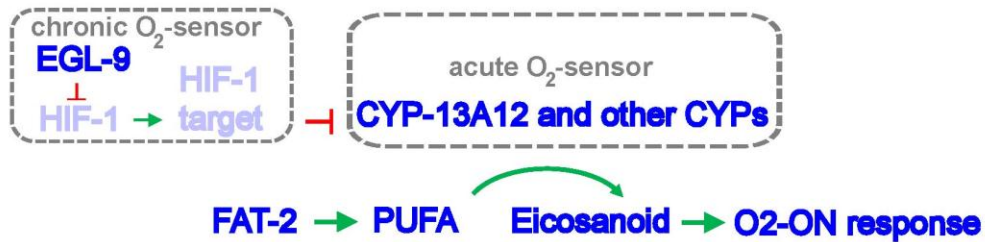


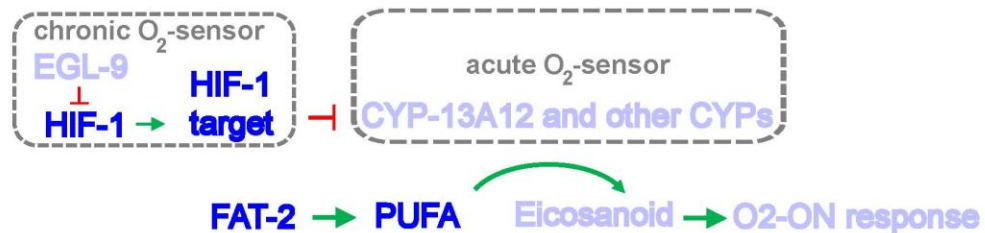
**fig. S7. The O<sub>2</sub>-ON response requires C20 PUFA biosynthesis**

(A) A schematic of a PUFA biosynthetic pathway showing biochemical functions of FAT-2 and FAT-3. Note that *fat-2* and *fat-3* mutants completely lack C20 PUFAs. (B) Speed graph of *fat-3* null mutants, showing a defective O<sub>2</sub>-ON response. Animals were supplemented with PUFA solvents used in (C) as a control. (C) Speed graph of *fat-3* mutants, showing the O<sub>2</sub>-ON response was rescued by C20 PUFA (arachidonic acid) supplementation. (D) Speed graph *fat-2* mutants, showing the O<sub>2</sub>-ON response was not rescued by supplementation with the C18 MUFA oleate.

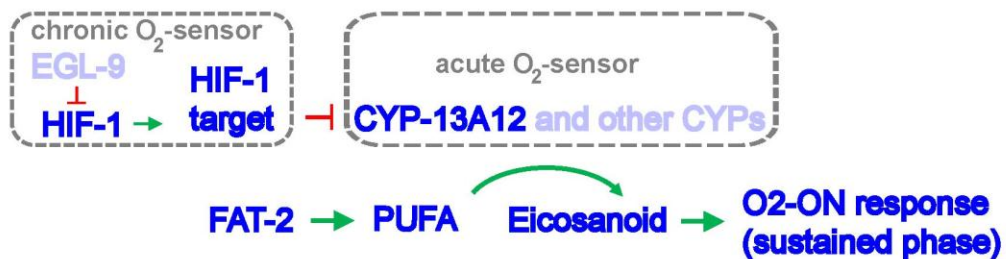
**A** Normal behavioral state in wild type



**B** Behavioral state in *egl-9* mutants or wild-type animals after hypoxic preconditioning



**C** Behavioral state in *egl-9; cyp-13A12(n5590)* mutants



**D** Behavioral state in *cyp-13A12* loss-of-function mutants

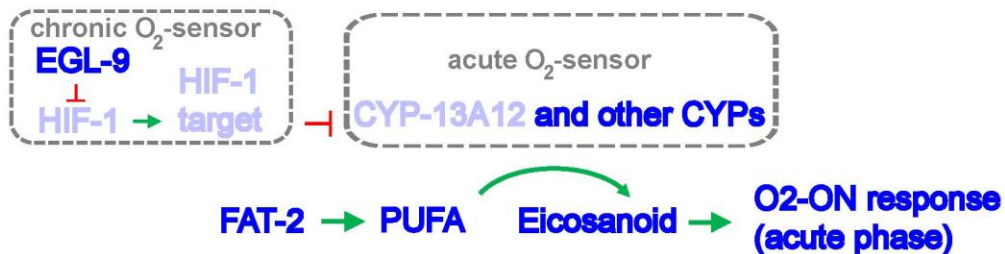
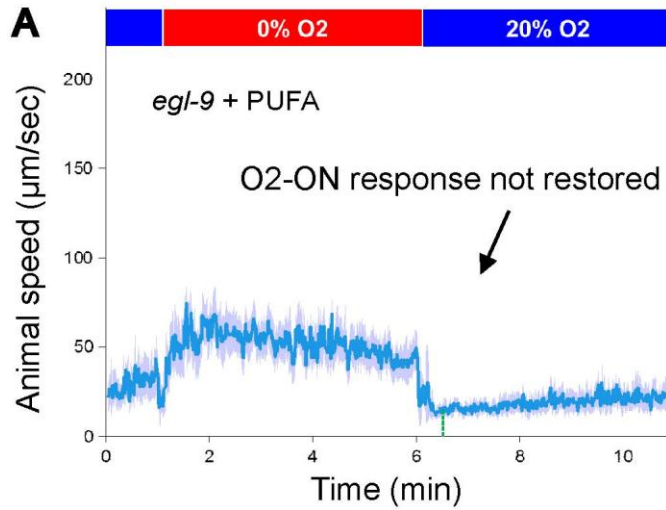


**fig. S8. Model for the control of the O<sub>2</sub>-ON response by EGL-9, CYPs and PUFAs.**

(A) Model for the molecular pathway by which EGL-9, CYP, PUFA-eicosanoids coordinately control the O<sub>2</sub>-ON response under normal conditions. CYP enzymes, including the PUFA oxygenase CYP-13A12, act as acute molecular O<sub>2</sub>-sensors during reoxygenation to promote the O<sub>2</sub>-ON response. The HIF hydroxylase EGL-9, by contrast, acts as a chronic O<sub>2</sub> sensor to suppress the O<sub>2</sub>-ON response by hypoxic preconditioning (10) via regulation of CYPs. The regulation of CYP-13A12 by HIF-1 occurs primarily at the protein level, likely via an unidentified HIF-1 transcriptional target that decreases CYP-13A12 protein levels. The biosynthesis of PUFAs, known physiological substrates of CYP enzymes, is mediated by the FAT-2 and FAT-3 lipid desaturases in a parallel pathway. The defective O<sub>2</sub>-ON response of *egl-9* mutants is not caused by a reduced activity of the FAT-2/FAT-3/PUFA pathway (fig. S9A); furthermore, HIF-1 activation might enhance but not reduce PUFA biosynthesis (70). In panels (A) - (D), the light blue indicates low levels of protein activity, eicosanoids, or a failure of the O<sub>2</sub>-ON response. (B) *egl-9* mutation causes HIF-1 activation and down-regulation of CYP-13A12 and other CYPs, resulting in a down-regulation of eicosanoids and suppression of the O<sub>2</sub>-ON response. (C) The gain-of-function mutation *cyp-13A12(n5590)* restores eicosanoid levels, leading to restoration of the sustained phase of the defective O<sub>2</sub>-ON response of *egl-9* mutants. In contrast to *cyp-13A12*, over-expression of another CYP gene *cyp-29A3* did not restore the defective O<sub>2</sub>-ON response in *egl-9* mutants (figs. S10A-S10B), indicating that restoration of the O<sub>2</sub>-ON response in *egl-9* mutants by *cyp-13A12(n5590)* is not caused by a general increased function of

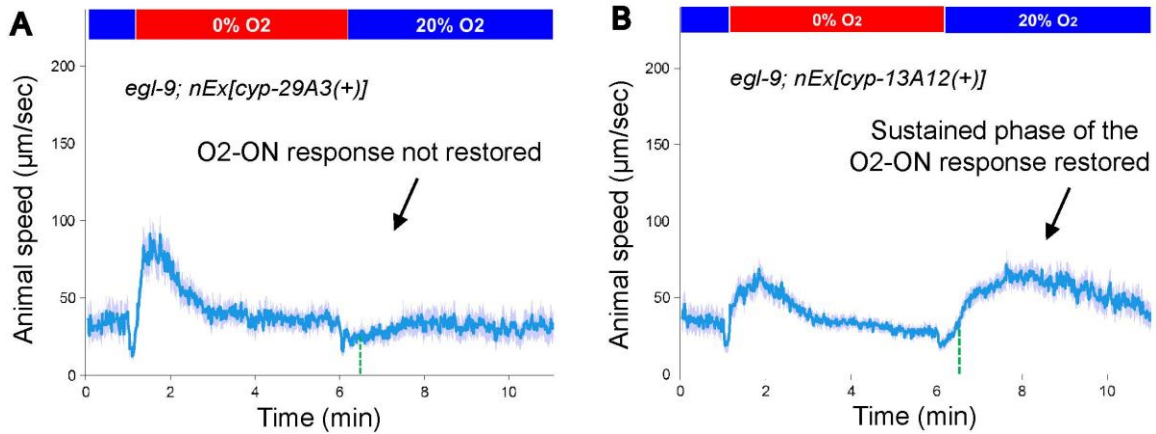
PUFA oxygenases. (D) The loss-of-function mutation *cyp-13A12(gk733685)* causes a specific defect in the sustained phase of the O<sub>2</sub>-ON response.

fig. S9



**fig. S9. The defective O<sub>2</sub>-ON response of *egl-9* mutants is not caused by a constitutive deficiency in PUFAs.**

(A) Speed graph of *egl-9* mutants, showing the defective O<sub>2</sub>-ON response was not rescued by exogenous C20 PUFA (arachidonic acid) as a dietary supplement.



**fig. S10. Specificity of CYP-13A12 in rescuing the O<sub>2</sub>-ON response by *egl-9* mutants.**

(A) Speed graph of *egl-9* mutants, showing the defective O<sub>2</sub>-ON response was not rescued by overexpression of *cyp-29A3(+)*. (B) Speed graph of *egl-9* mutants, showing the defective O<sub>2</sub>-ON response was rescued by overexpression of *cyp-13A12(+)* in the sustained but not the initial phase. The mean speed within 30-120 s after O<sub>2</sub> restoration is significantly higher than that of *egl-9(n586)* mutants ( $p < 0.01$ ).

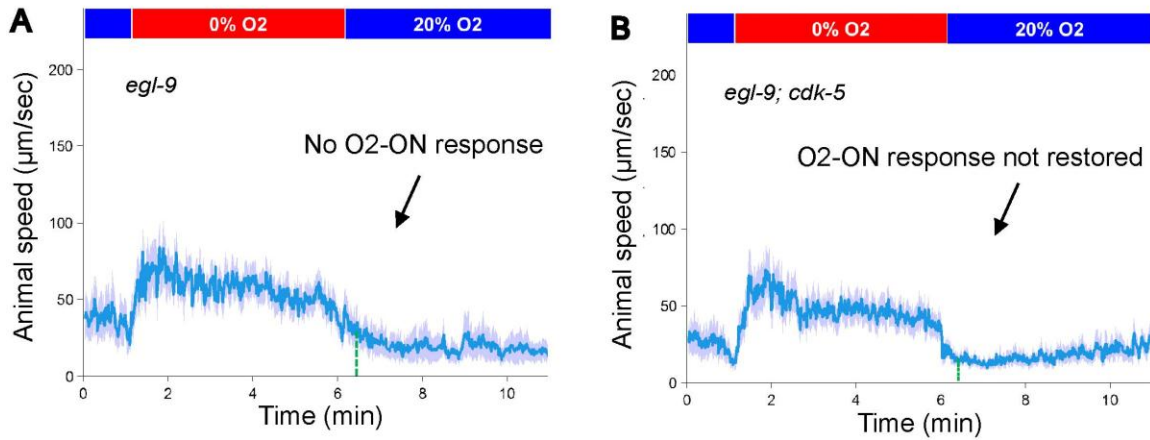


**fig. S11. EGL-9 and CYPs regulate the O<sub>2</sub>-ON response independently of CDK-5.**

(A) Speed graph of *egl-9* mutants, showing a defective O<sub>2</sub>-ON response. (B) Speed graph of *egl-9;cdk-5* mutants, showing the defective O<sub>2</sub>-ON response was not rescued by loss of *cdk-5*.

### Supplementary Table S1

(A) Protein-coding mutations within the genetically mapped interval identified by whole-genome sequencing of the *n5590* mutant. These mutations seen after EMS mutagenesis were not present in the parental mutagenized strain.

L G	Position	Ref. base	Sample base	Coverage	Mutation type	Codon change	Affected gene
III	12953211	T	G	6X	missense	AAT- >ACT [Asn->Thr]	<i>Y39E4A.2</i>
III	13024707	G	A	10X	missense	ATG- >ATA [Met->Ile]	<i>F14F7.3</i> ( <i>cyp-13A12</i> )
III	13050495	G	A	8X	silent	AAC- >AAT [Asn->Asn]	<i>F54F12.1</i>
III	13303608	G	A	13X	silent	CGC- >CGT [Arg->Arg]	<i>Y43F4B.6</i>

(B) Primers used for molecular cloning and the construction of transgenes

---

Primer name	Primer sequence
DM1377_cyp-13A12 g5p	TGCTTCTTAAAAGTCTGTAGAACCAAT
DM1378_cyp-13A12 g3p	GGTTTGCTGATTTGCCATTT
DM1391_cyp-13A12 nested c5p	tcaaaaattaaagccagcgtct
DM1392_cyp-13A12Pro to GFP c3p	CGACCTGCAGGCATGCAAGCTtttttaaactcaa aacttgaatggtc
DM1393_cyp-13A12Procod to GFP c3p	CAGTGAAAAGTTCTTCTCCTTTACTCAT ATTATCATCCCTCGGCGTCA
DM1503_cyp-13A12codutr Nested3p	GCTGATTTGCCATTTTGAAATT

---

## References

1. A. S. Go *et al.*, Heart disease and stroke statistics—2013 update. *Circulation* **127**, e6–e245 (2013). [doi:10.1161/CIR.0b013e31828124ad](https://doi.org/10.1161/CIR.0b013e31828124ad)
2. H. K. Eltzschig, T. Eckle, Ischemia and reperfusion—from mechanism to translation. *Nat. Med.* **17**, 1391–1401 (2011). [doi:10.1038/nm.2507](https://doi.org/10.1038/nm.2507) [Medline](#)
3. A. C. Epstein, J. M. Gleadle, L. A. McNeill, K. S. Hewitson, J. O'Rourke, D. R. Mole, M. Mukherji, E. Metzen, M. I. Wilson, A. Dhanda, Y. M. Tian, N. Masson, D. L. Hamilton, P. Jaakkola, R. Barstead, J. Hodgkin, P. H. Maxwell, C. W. Pugh, C. J. Schofield, P. J. Ratcliffe, *C. elegans* EGL-9 and mammalian homologs define a family of dioxygenases that regulate HIF by prolyl hydroxylation. *Cell* **107**, 43–54 (2001). [doi:10.1016/S0092-8674\(01\)00507-4](https://doi.org/10.1016/S0092-8674(01)00507-4) [Medline](#)
4. W. G. Kaelin Jr., P. J. Ratcliffe, Oxygen sensing by metazoans: The central role of the HIF hydroxylase pathway. *Mol. Cell* **30**, 393–402 (2008). [doi:10.1016/j.molcel.2008.04.009](https://doi.org/10.1016/j.molcel.2008.04.009) [Medline](#)
5. C. Trent, N. Tsuing, H. R. Horvitz, Egg-laying defective mutants of the nematode *Caenorhabditis elegans*. *Genetics* **104**, 619–647 (1983). [Medline](#)
6. G. L. Semenza, Hypoxia-inducible factors in physiology and medicine. *Cell* **148**, 399–408 (2012). [doi:10.1016/j.cell.2012.01.021](https://doi.org/10.1016/j.cell.2012.01.021) [Medline](#)
7. J. A. Powell-Coffman, Hypoxia signaling and resistance in *C. elegans*. *Trends Endocrinol. Metab.* **21**, 435–440 (2010). [doi:10.1016/j.tem.2010.02.006](https://doi.org/10.1016/j.tem.2010.02.006) [Medline](#)
8. G. L. Semenza, Hypoxia-inducible factor 1: Regulator of mitochondrial metabolism and mediator of ischemic preconditioning. *Biochim. Biophys. Acta* **1813**, 1263–1268 (2011). [doi:10.1016/j.bbamcr.2010.08.006](https://doi.org/10.1016/j.bbamcr.2010.08.006) [Medline](#)
9. J. Aragonés, M. Schneider, K. Van Geyte, P. Fraisl, T. Dresselaers, M. Mazzone, R. Dirx, S. Zacchigna, H. Lemieux, N. H. Jeoung, D. Lambrechts, T. Bishop, P. Lafuste, A. Diez-Juan, S. K. Harten, P. Van Noten, K. De Bock, C. Willam, M. Tjwa, A. Grosfeld, R. Navet, L. Moons, T. Vandendriessche, C. Deroose, B. Wijeyekoon, J. Nuyts, B. Jordan, R. Silasi-Mansat, F. Lupu, M. Dewerchin, C. Pugh, P. Salmon, L. Mortelmans, B. Gallez,

- F. Gorus, J. Buyse, F. Sluse, R. A. Harris, E. Gnaiger, P. Hespel, P. Van Hecke, F. Schuit, P. Van Veldhoven, P. Ratcliffe, M. Baes, P. Maxwell, P. Carmeliet, Deficiency or inhibition of oxygen sensor Phd1 induces hypoxia tolerance by reprogramming basal metabolism. *Nat. Genet.* **40**, 170–180 (2008). [doi:10.1038/ng.2007.62](https://doi.org/10.1038/ng.2007.62) [Medline](#)
10. D. K. Ma, R. Vozdek, N. Bhatla, H. R. Horvitz, CYSL-1 interacts with the O<sub>2</sub>-sensing hydroxylase EGL-9 to promote H<sub>2</sub>S-modulated hypoxia-induced behavioral plasticity in *C. elegans*. *Neuron* **73**, 925–940 (2012). [doi:10.1016/j.neuron.2011.12.037](https://doi.org/10.1016/j.neuron.2011.12.037) [Medline](#)
11. D. K. Ma, N. Ringstad, The neurobiology of sensing respiratory gases for the control of animal behavior. *Front. Biol.* **7**, 246–253 (2012). [doi:10.1007/s11515-012-1219-x](https://doi.org/10.1007/s11515-012-1219-x) [Medline](#)
12. M. W. Budde, M. B. Roth, The response of *Caenorhabditis elegans* to hydrogen sulfide and hydrogen cyanide. *Genetics* **189**, 521–532 (2011). [doi:10.1534/genetics.111.129841](https://doi.org/10.1534/genetics.111.129841) [Medline](#)
13. D. R. Nelson, L. Koymans, T. Kamataki, J. J. Stegeman, R. Feyereisen, D. J. Waxman, M. R. Waterman, O. Gotoh, M. J. Coon, R. W. Estabrook, I. C. Gunsalus, D. W. Nebert, P450 superfamily: Update on new sequences, gene mapping, accession numbers and nomenclature. *Pharmacogenetics* **6**, 1–42 (1996). [doi:10.1097/00008571-199602000-00002](https://doi.org/10.1097/00008571-199602000-00002) [Medline](#)
14. O. Gotoh, Divergent structures of *Caenorhabditis elegans* cytochrome P450 genes suggest the frequent loss and gain of introns during the evolution of nematodes. *Mol. Biol. Evol.* **15**, 1447–1459 (1998). [doi:10.1093/oxfordjournals.molbev.a025872](https://doi.org/10.1093/oxfordjournals.molbev.a025872) [Medline](#)
15. R. A. Gottlieb, Cytochrome P450: Major player in reperfusion injury. *Arch. Biochem. Biophys.* **420**, 262–267 (2003). [doi:10.1016/j.abb.2003.07.004](https://doi.org/10.1016/j.abb.2003.07.004) [Medline](#)
16. M. Kosel, W. Wild, A. Bell, M. Rothe, C. Lindschau, C. E. Steinberg, W. H. Schunck, R. Menzel, Eicosanoid formation by a cytochrome P450 isoform expressed in the pharynx of *Caenorhabditis elegans*. *Biochem. J.* **435**, 689–700 (2011). [doi:10.1042/BJ20101942](https://doi.org/10.1042/BJ20101942) [Medline](#)

17. J. Kulas, C. Schmidt, M. Rothe, W. H. Schunck, R. Menzel, Cytochrome P450-dependent metabolism of eicosapentaenoic acid in the nematode *Caenorhabditis elegans*. *Arch. Biochem. Biophys.* **472**, 65–75 (2008). [doi:10.1016/j.abb.2008.02.002](https://doi.org/10.1016/j.abb.2008.02.002) [Medline](#)
18. B. S. Berlett, E. R. Stadtman, Protein oxidation in aging, disease, and oxidative stress. *J. Biol. Chem.* **272**, 20313–20316 (1997). [doi:10.1074/jbc.272.33.20313](https://doi.org/10.1074/jbc.272.33.20313) [Medline](#)
19. R. C. Zangar, D. R. Davydov, S. Verma, Mechanisms that regulate production of reactive oxygen species by cytochrome P450. *Toxicol. Appl. Pharmacol.* **199**, 316–331 (2004). [doi:10.1016/j.taap.2004.01.018](https://doi.org/10.1016/j.taap.2004.01.018) [Medline](#)
20. C. A. Rappleye, A. Tagawa, N. Le Bot, J. Ahringer, R. V. Aroian, Involvement of fatty acid pathways and cortical interaction of the pronuclear complex in *Caenorhabditis elegans* embryonic polarity. *BMC Dev. Biol.* **3**, 8 (2003). [doi:10.1186/1471-213X-3-8](https://doi.org/10.1186/1471-213X-3-8) [Medline](#)
21. J. Szeffel, M. Piotrowska, W. J. Kruszewski, J. Jankun, W. Łysiak-Szydłowska, E. Skrzypczak-Jankun, Eicosanoids in prevention and management of diseases. *Curr. Mol. Med.* **11**, 13–25 (2011). [doi:10.2174/156652411794474374](https://doi.org/10.2174/156652411794474374) [Medline](#)
22. M. P. Wymann, R. Schneider, Lipid signalling in disease. *Nat. Rev. Mol. Cell Biol.* **9**, 162–176 (2008). [doi:10.1038/nrm2335](https://doi.org/10.1038/nrm2335) [Medline](#)
23. R. S. Chapkin, W. Kim, J. R. Lupton, D. N. McMurray, Dietary docosahexaenoic and eicosapentaenoic acid: Emerging mediators of inflammation. *Prostaglandins Leukot. Essent. Fatty Acids* **81**, 187–191 (2009). [doi:10.1016/j.plefa.2009.05.010](https://doi.org/10.1016/j.plefa.2009.05.010) [Medline](#)
24. D. Panigrahy, A. Kaipainen, E. R. Greene, S. Huang, Cytochrome P450-derived eicosanoids: The neglected pathway in cancer. *Cancer Metastasis Rev.* **29**, 723–735 (2010). [doi:10.1007/s10555-010-9264-x](https://doi.org/10.1007/s10555-010-9264-x) [Medline](#)
25. C. Arnold, M. Markovic, K. Blossey, G. Wallukat, R. Fischer, R. Dechend, A. Konkel, C. von Schacky, F. C. Luft, D. N. Muller, M. Rothe, W. H. Schunck, Arachidonic acid-metabolizing cytochrome P450 enzymes are targets of omega-3 fatty acids. *J. Biol. Chem.* **285**, 32720–32733 (2010). [doi:10.1074/jbc.M110.118406](https://doi.org/10.1074/jbc.M110.118406) [Medline](#)
26. J. L. Watts, Fat synthesis and adiposity regulation in *Caenorhabditis elegans*. *Trends Endocrinol. Metab.* **20**, 58–65 (2009). [doi:10.1016/j.tem.2008.11.002](https://doi.org/10.1016/j.tem.2008.11.002) [Medline](#)

27. D. R. Harder, J. Narayanan, E. K. Birks, J. F. Liard, J. D. Imig, J. H. Lombard, A. R. Lange, R. J. Roman, Identification of a putative microvascular oxygen sensor. *Circ. Res.* **79**, 54–61 (1996). [doi:10.1161/01.RES.79.1.54](https://doi.org/10.1161/01.RES.79.1.54) [Medline](#)
28. J. P. Ward, Oxygen sensors in context. *Biochim. Biophys. Acta* **1777**, 1–14 (2008). [doi:10.1016/j.bbabi.2007.10.010](https://doi.org/10.1016/j.bbabi.2007.10.010) [Medline](#)
29. M. Gerber, Omega-3 fatty acids and cancers: A systematic update review of epidemiological studies. *Br. J. Nutr.* **107** (suppl. 2), S228–S239 (2012). [doi:10.1017/S0007114512001614](https://doi.org/10.1017/S0007114512001614) [Medline](#)
30. D. Mozaffarian, J. H. Wu, Omega-3 fatty acids and cardiovascular disease: Effects on risk factors, molecular pathways, and clinical events. *J. Am. Coll. Cardiol.* **58**, 2047–2067 (2011). [doi:10.1016/j.jacc.2011.06.063](https://doi.org/10.1016/j.jacc.2011.06.063) [Medline](#)
31. L. Avery, J. H. Thomas, Feeding and defecation. In *C. elegans II*, D. L. Riddle, T. Blumenthal, B. J. Meyer, J. R. Priess, Eds. (Cold Spring Harbor Laboratory Press, Cold Spring Harbor, NY, 2011), chap. 24.
32. Z. F. Altun, D. H. Hall, in *WormAtlas*, L. A. Herndon, Ed.; [www.wormatlas.org](http://www.wormatlas.org).
33. K. E. Busch, P. Laurent, Z. Soltesz, R. J. Murphy, O. Faivre, B. Hedwig, M. Thomas, H. L. Smith, M. de Bono, Tonic signaling from O<sub>2</sub> sensors sets neural circuit activity and behavioral state. *Nat. Neurosci.* **15**, 581–591 (2012). [doi:10.1038/nn.3061](https://doi.org/10.1038/nn.3061) [Medline](#)
34. M. Zimmer, J. M. Gray, N. Pokala, A. J. Chang, D. S. Karow, M. A. Marletta, M. L. Hudson, D. B. Morton, N. Chronis, C. I. Bargmann, Neurons detect increases and decreases in oxygen levels using distinct guanylate cyclases. *Neuron* **61**, 865–879 (2009). [doi:10.1016/j.neuron.2009.02.013](https://doi.org/10.1016/j.neuron.2009.02.013) [Medline](#)
35. J. M. Gray, D. S. Karow, H. Lu, A. J. Chang, J. S. Chang, R. E. Ellis, M. A. Marletta, C. I. Bargmann, Oxygen sensation and social feeding mediated by a *C. elegans* guanylate cyclase homologue. *Nature* **430**, 317–322 (2004). [doi:10.1038/nature02714](https://doi.org/10.1038/nature02714) [Medline](#)
36. M. de Bono, A. V. Maricq, Neuronal substrates of complex behaviors in *C. elegans*. *Annu. Rev. Neurosci.* **28**, 451–501 (2005). [doi:10.1146/annurev.neuro.27.070203.144259](https://doi.org/10.1146/annurev.neuro.27.070203.144259) [Medline](#)

37. B. J. Piggott, J. Liu, Z. Feng, S. A. Wescott, X. Z. Xu, The neural circuits and synaptic mechanisms underlying motor initiation in *C. elegans*. *Cell* **147**, 922–933 (2011).  
[doi:10.1016/j.cell.2011.08.053](https://doi.org/10.1016/j.cell.2011.08.053) [Medline](#)
38. R. Mehta, K. A. Steinkraus, G. L. Sutphin, F. J. Ramos, L. S. Shamieh, A. Huh, C. Davis, D. Chandler-Brown, M. Kaeberlein, Proteasomal regulation of the hypoxic response modulates aging in *C. elegans*. *Science* **324**, 1196–1198 (2009).  
[doi:10.1126/science.1173507](https://doi.org/10.1126/science.1173507)
39. X. R. Mao, C. M. Crowder, Protein misfolding induces hypoxic preconditioning via a subset of the unfolded protein response machinery. *Mol. Cell. Biol.* **30**, 5033–5042 (2010).  
[doi:10.1128/MCB.00922-10](https://doi.org/10.1128/MCB.00922-10) [Medline](#)
40. D. L. Miller, M. W. Budde, M. B. Roth, HIF-1 and SKN-1 coordinate the transcriptional response to hydrogen sulfide in *Caenorhabditis elegans*. *PLoS ONE* **6**, e25476 (2011).  
[doi:10.1371/journal.pone.0025476](https://doi.org/10.1371/journal.pone.0025476) [Medline](#)
41. E. C. Park, P. Ghose, Z. Shao, Q. Ye, L. Kang, X. Z. Xu, J. A. Powell-Coffman, C. Rongo, Hypoxia regulates glutamate receptor trafficking through an HIF-independent mechanism. *EMBO J.* **31**, 1379–1393 (2012). [doi:10.1038/emboj.2011.499](https://doi.org/10.1038/emboj.2011.499) [Medline](#)
42. I. M. Booth Depaz, F. Toselli, P. A. Wilce, E. M. Gillam, Differential expression of human cytochrome P450 enzymes from the CYP3A subfamily in the brains of alcoholic subjects and drug-free controls. *Drug Metab. Dispos.* **41**, 1187–1194 (2013).  
[doi:10.1124/dmd.113.051359](https://doi.org/10.1124/dmd.113.051359) [Medline](#)
43. C. Ghosh, N. Marchi, N. K. Desai, V. Puvenna, M. Hossain, J. Gonzalez-Martinez, A. V. Alexopoulos, D. Janigro, Cellular localization and functional significance of CYP3A4 in the human epileptic brain. *Epilepsia* **52**, 562–571 (2011). [doi:10.1111/j.1528-1167.2010.02956.x](https://doi.org/10.1111/j.1528-1167.2010.02956.x) [Medline](#)
44. V. Agarwal, R. P. Kommaddi, K. Valli, D. Ryder, T. M. Hyde, J. E. Kleinman, H. W. Strobel, V. Ravindranath, Drug metabolism in human brain: High levels of cytochrome P4503A43 in brain and metabolism of anti-anxiety drug alprazolam to its active metabolite. *PLoS ONE* **3**, e2337 (2008). [doi:10.1371/journal.pone.0002337](https://doi.org/10.1371/journal.pone.0002337) [Medline](#)

45. A. Gabrielsen, H. Qiu, M. Bäck, M. Hamberg, A. L. Hemdahl, H. Agardh, L. Folkersen, J. Swedenborg, U. Hedin, G. Paulsson-Berne, J. Z. Haeggström, G. K. Hansson, Thromboxane synthase expression and thromboxane A2 production in the atherosclerotic lesion. *J. Mol. Med.* **88**, 795–806 (2010). [doi:10.1007/s00109-010-0621-6](https://doi.org/10.1007/s00109-010-0621-6) [Medline](#)
46. T. Kawasaki, T. Marumo, K. Shirakami, T. Mori, H. Doi, M. Suzuki, Y. Watanabe, S. Chaki, A. Nakazato, Y. Ago, H. Hashimoto, T. Matsuda, A. Baba, H. Onoe, Increase of 20-HETE synthase after brain ischemia in rats revealed by PET study with <sup>11</sup>C-labeled 20-HETE synthase-specific inhibitor. *J. Cereb. Blood Flow Metab.* **32**, 1737–1746 (2012). [doi:10.1038/jcbfm.2012.68](https://doi.org/10.1038/jcbfm.2012.68) [Medline](#)
47. K. M. Dunn, M. Renic, A. K. Flasch, D. R. Harder, J. Falck, R. J. Roman, Elevated production of 20-HETE in the cerebral vasculature contributes to severity of ischemic stroke and oxidative stress in spontaneously hypertensive rats. *Am. J. Physiol. Heart Circ. Physiol.* **295**, H2455–H2465 (2008). [doi:10.1152/ajpheart.00512.2008](https://doi.org/10.1152/ajpheart.00512.2008) [Medline](#)
48. Y. Ishihara, M. Sekine, M. Nakazawa, N. Shimamoto, Suppression of myocardial ischemia-reperfusion injury by inhibitors of cytochrome P450 in rats. *Eur. J. Pharmacol.* **611**, 64–71 (2009). [doi:10.1016/j.ejphar.2009.03.069](https://doi.org/10.1016/j.ejphar.2009.03.069) [Medline](#)
49. M. Khan, I. K. Mohan, V. K. Kutala, D. Kumbala, P. Kuppusamy, Cardioprotection by sulfaphenazole, a cytochrome p450 inhibitor: Mitigation of ischemia-reperfusion injury by scavenging of reactive oxygen species. *J. Pharmacol. Exp. Ther.* **323**, 813–821 (2007). [doi:10.1124/jpet.107.129486](https://doi.org/10.1124/jpet.107.129486) [Medline](#)
50. M. W. Davis, M. Hammarlund, T. Harrach, P. Hullett, S. Olsen, E. M. Jorgensen, Rapid single nucleotide polymorphism mapping in *C. elegans*. *BMC Genomics* **6**, 118 (2005). [doi:10.1186/1471-2164-6-118](https://doi.org/10.1186/1471-2164-6-118)
51. S. Sarin, S. Prabhu, M. M. O’Meara, I. Pe’er, O. Hobert, *Caenorhabditis elegans* mutant allele identification by whole-genome sequencing. *Nat. Methods* **5**, 865–867 (2008). [doi:10.1038/nmeth.1249](https://doi.org/10.1038/nmeth.1249) [Medline](#)
52. N. Ringstad, H. R. Horvitz, FMRFamide neuropeptides and acetylcholine synergistically inhibit egg-laying by *C. elegans*. *Nat. Neurosci.* **11**, 1168–1176 (2008). [doi:10.1038/nn.2186](https://doi.org/10.1038/nn.2186) [Medline](#)

53. O. H. Lowry, N. J. Rosebrough, A. L. Farr, R. J. Randall, Protein measurement with the Folin phenol reagent. *J. Biol. Chem.* **193**, 265–275 (1951). [Medline](#)
54. S. Brenner, The genetics of *Caenorhabditis elegans*. *Genetics* **77**, 71–94 (1974). [Medline](#)
55. S. R. Wicks, R. T. Yeh, W. R. Gish, R. H. Waterston, R. H. Plasterk, Rapid gene mapping in *Caenorhabditis elegans* using a high density polymorphism map. *Nat. Genet.* **28**, 160–164 (2001). [doi:10.1038/88878](https://doi.org/10.1038/88878) [Medline](#)
56. S. Flibotte, M. L. Edgley, I. Chaudhry, J. Taylor, S. E. Neil, A. Rogula, R. Zapf, M. Hirst, Y. Butterfield, S. J. Jones, M. A. Marra, R. J. Barstead, D. G. Moerman, Whole-genome profiling of mutagenesis in *Caenorhabditis elegans*. *Genetics* **185**, 431–441 (2010). [doi:10.1534/genetics.110.116616](https://doi.org/10.1534/genetics.110.116616) [Medline](#)
57. J. L. Watts, J. Browse, *Proc. Natl. Acad. Sci. U.S.A.* **99**, 32 (2002).
58. C. Darby, C. L. Cosma, J. H. Thomas, C. Manoil, Lethal paralysis of *Caenorhabditis elegans* by *Pseudomonas aeruginosa*. *Proc. Natl. Acad. Sci. U.S.A.* **96**, 15202–15207 (1999). [doi:10.1073/pnas.96.26.15202](https://doi.org/10.1073/pnas.96.26.15202) [Medline](#)
59. C. Shen, D. Nettleton, M. Jiang, S. K. Kim, J. A. Powell-Coffman, Roles of the HIF-1 hypoxia-inducible factor during hypoxia response in *Caenorhabditis elegans*. *J. Biol. Chem.* **280**, 20580–20588 (2005). [doi:10.1074/jbc.M501894200](https://doi.org/10.1074/jbc.M501894200) [Medline](#)
60. H. Jiang, R. Guo, J. A. Powell-Coffman, The *Caenorhabditis elegans* hif-1 gene encodes a bHLH-PAS protein that is required for adaptation to hypoxia. *Proc. Natl. Acad. Sci. U.S.A.* **98**, 7916–7921 (2001). [doi:10.1073/pnas.141234698](https://doi.org/10.1073/pnas.141234698) [Medline](#)
61. C. C. Mello, J. M. Kramer, D. Stinchcomb, V. Ambros, Efficient gene transfer in *C. elegans*: Extrachromosomal maintenance and integration of transforming sequences. *EMBO J.* **10**, 3959–3970 (1991). [Medline](#)
62. T. Boulin, J. F. Etchberger, O. Hobert, Reporter gene fusions. *WormBook* 10.1895/wormbook.1.106.1 (2006). [doi:10.1895/wormbook.1.106.1](https://doi.org/10.1895/wormbook.1.106.1)
63. J. L. Hartley, G. F. Temple, M. A. Brasch, DNA cloning using in vitro site-specific recombination. *Genome Res.* **10**, 1788–1795 (2000). [doi:10.1101/gr.143000](https://doi.org/10.1101/gr.143000) [Medline](#)

64. S. F. Altschul, W. Gish, W. Miller, E. W. Myers, D. J. Lipman, Basic local alignment search tool. *J. Mol. Biol.* **215**, 403–410 (1990). [Medline](#)
65. M. A. Larkin, G. Blackshields, N. P. Brown, R. Chenna, P. A. McGettigan, H. McWilliam, F. Valentin, I. M. Wallace, A. Wilm, R. Lopez, J. D. Thompson, T. J. Gibson, D. G. Higgins, Clustal W and Clustal X version 2.0. *Bioinformatics* **23**, 2947–2948 (2007). [doi:10.1093/bioinformatics/btm404](https://doi.org/10.1093/bioinformatics/btm404) [Medline](#)
66. A. M. Waterhouse, J. B. Procter, D. M. Martin, M. Clamp, G. J. Barton, Jalview Version 2—a multiple sequence alignment editor and analysis workbench. *Bioinformatics* **25**, 1189–1191 (2009). [doi:10.1093/bioinformatics/btp033](https://doi.org/10.1093/bioinformatics/btp033) [Medline](#)
67. T. Hirokawa, S. Boon-Chieng, S. Mitaku, SOSUI: Classification and secondary structure prediction system for membrane proteins. *Bioinformatics* **14**, 378–379 (1998). [doi:10.1093/bioinformatics/14.4.378](https://doi.org/10.1093/bioinformatics/14.4.378) [Medline](#)
68. H. Y. Mak, G. Ruvkun, Intercellular signaling of reproductive development by the *C. elegans* DAF-9 cytochrome P450. *Development* **131**, 1777–1786 (2004). [doi:10.1242/dev.01069](https://doi.org/10.1242/dev.01069) [Medline](#)
69. D. L. Motola, C. L. Cummins, V. Rottiers, K. K. Sharma, T. Li, Y. Li, K. Suino-Powell, H. E. Xu, R. J. Auchus, A. Antebi, D. J. Mangelsdorf, Identification of ligands for DAF-12 that govern dauer formation and reproduction in *C. elegans*. *Cell* **124**, 1209–1223 (2006). [doi:10.1016/j.cell.2006.01.037](https://doi.org/10.1016/j.cell.2006.01.037) [Medline](#)
70. M. Xie, R. Roy, Increased levels of hydrogen peroxide induce a HIF-1-dependent modification of lipid metabolism in AMPK compromised *C. elegans* dauer larvae. *Cell Metab.* **16**, 322–335 (2012). [Medline](#)